

**University of Rhode Island  
DigitalCommons@URI**

---

Physical Oceanography Technical Reports

Physical Oceanography

---

1991

# Inverted Echo Sounder Telemetry System Report

Stephan Howden

Karen L. Tracey

*University of Rhode Island*, [krltracey@uri.edu](mailto:krltracey@uri.edu)

*See next page for additional authors*

Creative Commons License



This work is licensed under a [Creative Commons Attribution-Noncommercial-Share Alike 3.0 License](#).

Follow this and additional works at: [http://digitalcommons.uri.edu/  
physical\\_oceanography\\_techrpts](http://digitalcommons.uri.edu/physical_oceanography_techrpts)

---

## Recommended Citation

Howden, Stephan; Tracey, Karen L.; Watts, D. Randolph; and Rossby, H. Thomas, "Inverted Echo Sounder Telemetry System Report" (1991). *Physical Oceanography Technical Reports*. Paper 25.  
[http://digitalcommons.uri.edu/physical\\_oceanography\\_techrpts/25](http://digitalcommons.uri.edu/physical_oceanography_techrpts/25) [http://digitalcommons.uri.edu/physical\\_oceanography\\_techrpts/25](http://digitalcommons.uri.edu/physical_oceanography_techrpts/25)

This Article is brought to you for free and open access by the Physical Oceanography at DigitalCommons@URI. It has been accepted for inclusion in Physical Oceanography Technical Reports by an authorized administrator of DigitalCommons@URI. For more information, please contact [digitalcommons@etal.uri.edu](mailto:digitalcommons@etal.uri.edu).

---

**Authors**

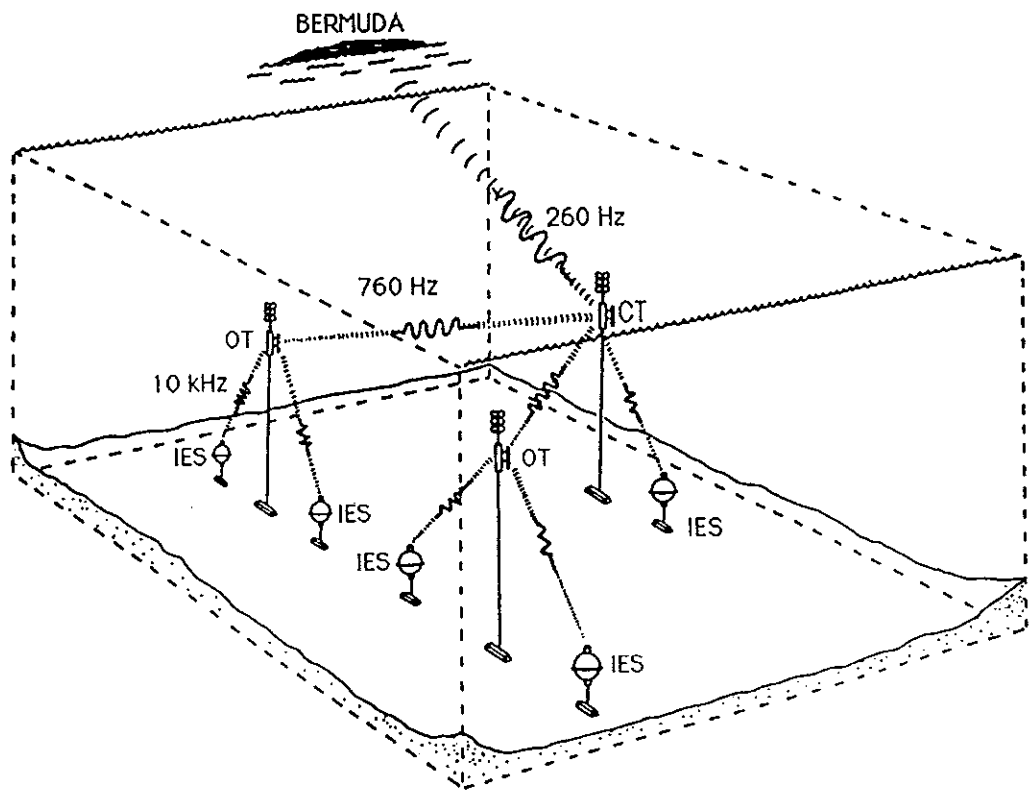
Stephan Howden, Karen L. Tracey, D. Randolph Watts, and H. Thomas Rossby

*Karen Tracey*

GRADUATE SCHOOL OF OCEANOGRAPHY  
UNIVERSITY OF RHODE ISLAND  
NARRAGANSETT, RHODE ISLAND

Inverted Echo Sounder  
Telemetry System Report

GSO Technical Report No. 91-8



by

Stephan Howden, Karen Tracey, D. Randolph Watts and H. Thomas Rossby

December

1991

This research program has been sponsored by the Office of Naval Research under contract

N00014-89J-1919.

### **Abstract**

From August 1989 until August 1990, a simple acoustic telemetry system was used for obtaining real-time data from 5 Inverted Echo Sounders (IESs) deployed in the SYNOP inlet array in the Gulf Stream east of Cape Hatteras. Every 24 hours, each IES calculated a representative travel time from a set of 48 measurements ( $\tau$ ), and telemetered that value to a listening station on Bermuda. From the received data, a daily time series of the depth of the 12°C isotherm (our proxy for main thermocline depth) over each IES was calculated. The position of the Gulf Stream North Wall through the IES array was calculated on a daily basis from the thermocline depth information at each IES site.

The telemetry system is based on encoding data as a time delayed broadcast acoustic signal: the delay of the time of broadcast of the signal, with respect to a reference time, is proportional to the data value. The changes in delay time, from one broadcast signal to the next, are recorded at a remote receiving station.

The IESs were recovered in August 1990, with the exception of the one at site B2. The telemetered data from the IES at site B2 was, however, received at Bermuda. The RMS agreement between thermocline depths, as calculated from the data on tape from the recovered IESs and as calculated from the received telemetry data, is 20 m. This compares favorably with the 19 m uncertainty in calibrating the  $\tau$ s as a measure of the thermocline depth. The RMS agreement between the position of the Gulf Stream path through the IESs as calculated from the tape data and the telemetry data is 5 km.

This telemetry system is not IES specific. It could be used with other appropriately modified oceanographic instruments, such as current meters and pressure sensors.

# Contents

<b>Abstract</b>	i
<b>List of Figures</b>	iv
<b>List of Tables</b>	iv
<b>1 Introduction</b>	1
<b>2 Telemetry System</b>	3
2.1 IES . . . . .	3
2.2 Transponders . . . . .	4
2.3 Base Station . . . . .	6
2.4 Signal Timing . . . . .	8
<b>3 Chronology</b>	8
<b>4 Data Representation: Telemetered And Taped</b>	11
<b>5 Processing</b>	14
5.1 Taped Data . . . . .	14
5.1.1 Calibration of $\tau$ to $Z_{12}$ . . . . .	16
5.1.2 Traditional Processing of Taped IES Data . . . . .	16
5.1.3 Reconstruction of the Telemetered Data . . . . .	17
5.2 Telemetered Data . . . . .	17
5.2.1 IES Clock-Drift Correction . . . . .	17
5.2.2 Calibration of $\tau$ to $Z_{12}$ . . . . .	22
5.2.3 Despike . . . . .	24
5.2.4 Seacor (Seasonal Thermocline Correction) . . . . .	25
5.2.5 $Z_{12}$ . . . . .	25
5.2.6 Fill-in . . . . .	25
5.2.7 Low-pass Filter . . . . .	26
<b>6 Results</b>	26
6.1 Data Return . . . . .	26
6.2 Data Acceptance . . . . .	27
6.3 Delay Time Comparison . . . . .	27
6.4 $Z_{12}$ Comparison . . . . .	27
6.5 Gulf Stream Position . . . . .	33

6.6 Telemetry System Problems . . . . .	34
<b>7 Summary and Conclusions</b>	<b>36</b>
<b>8 <u>References</u></b>	<b>37</b>

## List of Figures

1	IES telemetry map . . . . .	2
2	IES Data Aquisition And Internal Processing Flow Chart . . . . .	5
3	IES Acoustic Field Diagram . . . . .	6
4	Intermediate Transponder Mooring . . . . .	7
5	Bermuda Receiving Station . . . . .	9
6	Timing of Telemetered Signal . . . . .	10
7	Telemetry System and Rafos Navigation Schedule . . . . .	10
8	Data Word Manipulation . . . . .	13
9	Processing of Taped and Telemetered Data . . . . .	15
10	Processing: IES B2 . . . . .	18
11	Processing: IES B3 . . . . .	19
12	Processing: IES B4 . . . . .	20
13	Processing: IES B5 . . . . .	21
14	Drift Correction: IES B3 . . . . .	23
15	IES Total Data Return . . . . .	26
16	B3 Time Delay: Tape vs Telemetered . . . . .	28
17	B4 Time Delay: Tape vs Telemetered . . . . .	29
18	B5 Time Delay: Tape vs Telemetered . . . . .	30
19	Tape and Telemetry $Z_{12}$ Records . . . . .	32
20	Gulf Stream North Wall Position . . . . .	35

## List of Tables

1	Field Instrument Deployment and Recovery . . . . .	3
2	Telemetry Chronology . . . . .	11
3	<i>BDACT, NCT</i> and $\tau$ Conversions . . . . .	14
4	Bints and Drift Rates . . . . .	24
5	Tape vs Telemetry: rms Differences . . . . .	31
6	Tape vs Telemetry : rms of $Z_{12}$ Separately Processed . . . . .	33

## 1 Introduction

From August 1989 until August 1990, a system to acoustically telemeter data from five modified Inverted Echo Sounders (IESs) moored in the SYNOP Inlet Array was in operation. Figure 1 shows a map of the IES sites. All but one of the IESs were recovered during R/V Endeavor cruise EN216 in August 1990. Although the IES at site B2 was lost, its data was received at Bermuda throughout the year-long telemetry experiment. Regretfully, the IES at site C2 did not perform satisfactorily so neither the telemetered nor the recorded data were usable.

The telemetry scheme is based on the simple idea of encoding the IES travel time, the time ( $\tau$ ) taken for an acoustic signal to travel to the ocean surface and back to the bottom-moored IES, as a time delayed telemetered signal. That is, the amount of delay time relative to some reference time, is directly proportional to  $\tau$ .

In order to implement the telemetry scheme three basic requirements are needed. The first is an IES that can internally process the  $\tau$ s to encode them as a delay time and then transmit the encoded signal. The second is a mid-sound-channel relay station to receive the telemetered signals from the IESs and retransmit them to the final requirement, the distant shore-based receiving station.

The telemetry system was relatively easy to construct since the basic components already existed and required only relatively minor modifications. The IESs are already microprocessor controlled and are available with hardware options (described below) which meet the systems needs. The intermediate transponders/receivers were constructed from SOFAR sound sources modified to receive as well as transmit signals. The base station was also already operational as a listening station for the SOFAR sound sources used in Tom Rossby's Gulf Stream RAFOS float program and needed only a receiver and microprocessor that could detect, decode, and store telemetry signals and forward them through a modem upon demand.

This report gives a complete description of the telemetry system and its successful application as a source of real-time  $Z_{12}$  measurements from four IESs moored along a line perpendicular to the mean Gulf Stream path. Hence, the telemetry system was a source of real-time measurements of the GSNW position through the IES array. The order of presentation in this report is to first, describe the telemetry system; second, present a chronology for the experiment; third, give a discussion of the different methods of data representation (data words) for the internal processor of the IES, the data written to tape, and the telemetered data; fourth, describe the data processing for both taped and telemetered data; fifth, give a results section; sixth, summarize the problems encountered in the experiment and discuss how they may be avoided in future experiments; and finally, present a summary and conclusions section.

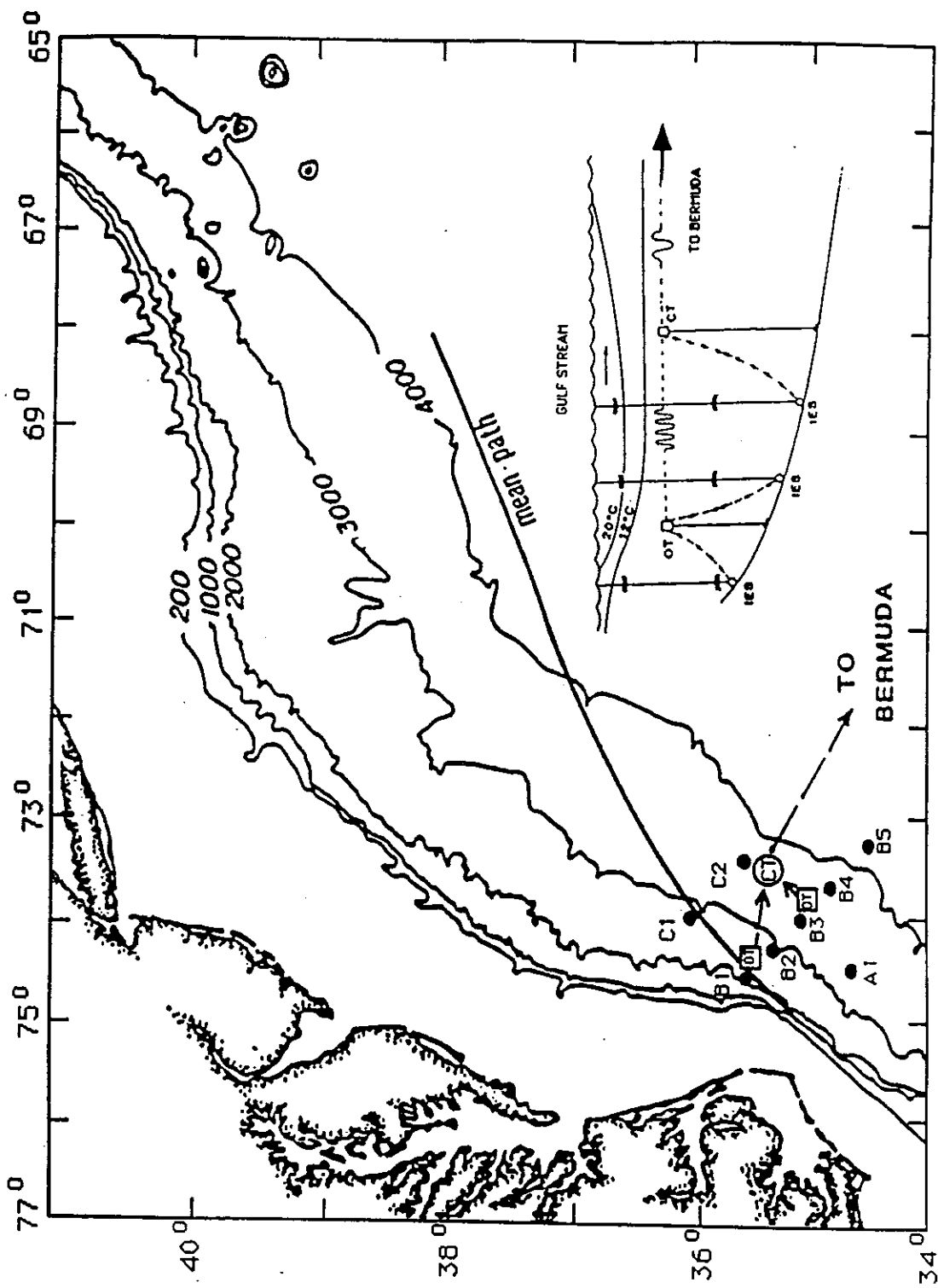


Figure 1: Location and telemetry arrangement of the five IESs in the SYNOP inlet array off of Cape Hatteras. The inset is a schematic of the data relay system.

## 2 Telemetry System

The telemetry system consisted of four parts: the modified IESs, the overhead and central transponders, the receiving station at Bermuda, and the acoustic hook up (via modems) between Bermuda and the University of Rhode Island (URI). Table 1 lists the deployment and recovery information about the field instruments of the telemetry system. The inset of Figure 1 shows schematically how the system works.

The basic telemetry scheme transmitted a signal from the IESs to Bermuda via some intermediary receivers/transponders moored in the SOFAR channel. The data were encoded as a time-delayed signal proportional to a daily averaged  $\tau$ .

Table 1: Field instrument deployment and recovery information. The signals from the original IES at site C2 (IES C2') interfered with those from the IESs at sites B2 and B5. The IES with which it was replaced (IES C2) did not function properly.

Instrument Site	Deployment			Recovery			Lat (N)	Lon (W)	Depth (m)
	Date (Z)	Time (Z)	Cruise ID	Date (Z)	Time (Z)	Cruise ID			
IES C2'	08/12/89	1717	OC210	10/17/89	0721	CH	35 46.15	73 33.00	3450
IES C2	10/17/89	1015	CH	09/03/90	0225	EN216	35 46.22	73 32.75	~3353
IES B2	08/10/89	0510	OC210			Not Recovered	35 37.01	74 13.82	2675
IES B3	08/10/89	0932	OC210	09/02/90	1250	EN216	35 30.07	74 03.40	2960
IES B4	08/11/89	1859	OC210	09/02/90	1551	EN216	35 20.75	74 50.60	3325
IES B5	08/11/89	1515	OC210	09/02/90	1835	EN216	35 12.13	73 39.66	3675
CT1	08/29/89	1907	OC210	08/29/90	0026	EN216	35 44.67	73 35.47	3480
OT1	08/30/89	0416	OC210	08/28/90	1558	EN216	35 32.80	74 06.20	2870
OT2	08/30/89	1641	OC210	08/28/90	2011	EN216	35 16.85	73 44.10	3500

### 2.1 IES

Inverted Echo Sounders are devices which emit and receive acoustic signals. They are moored one meter above the ocean floor and are designed to transmit acoustic signals towards the ocean surface, receive the reflected signal and record the round-trip travel time. The IES concept is described in Watts and Rossby (1976).

The traditional data acquisition scheme of the IESs follows the procedure described below. Every half-hour an IES transmits a burst of 24 10-kHz acoustic signals at 10 s intervals. The receiver blocks out early returns: i.e., any signals which may arrive before a time interval (preselected by the user) that is less than the shortest time interval for sound to travel to the surface and back. In a twenty-four hour period, 48 sample bursts of 24 pings (a total of 1152  $\tau$ s) are written to tape.

In addition to the data acquisition and internal processing scheme described above, the telemetry IESs did further internal processing of the data in order to put it in a form suitable for the telemetry system. Due primarily to power limitations of the transponders, only one signal per day was sent

from each IES to the base station at Bermuda. Thus, the IES microprocessor was programmed to calculate one representative value from the daily set of measured  $\tau_s$ . For each half hourly burst of 24 signals, the microprocessor stored in an accumulator the value  $\tau_{1q}$ , which corresponded to the first-quartile point in the distribution of the  $\tau_s$ . The value  $\tau_{1q}$  was also written to tape along with the 24  $\tau_s$  from that burst. The daily representative  $\tau$  was calculated after each 24 hrs as the mean of the 48 values of  $\tau_{1q}$  stored in the accumulator ( $\bar{\tau}_{1q}$ ). This daily representative travel time was encoded as a time-delayed acoustic signal and sent to a relay transponder.

A flow chart of the data acquisition scheme is shown in Figure 2. The optional hardware chosen for the Pacer Systems Inc. Model 1665 IESs used in the deployment included:

- The high output driver and transducer option to ensure that the telemetered signal would reach an intermediate transponder (the horizontal component of the signal is larger with this option).
- The 50,000  $\mu$ fd capacitor option and high current capacity lithium batteries were used to ensure sufficient power while transmitting the telemetered signal (50 ms transmission duration).

## 2.2 Transponders

The IES is not designed to send acoustic signals over long horizontal distances. Its high frequency acoustic signals are inefficient for long range propagation. Moreover, moored near the sea floor, the IES is not positioned for its signals to take advantage of the SOFAR channel. As illustrated in Figure 3, when moored at a nominal depth of 4500 m the IES's 10-kHz acoustic signal has a horizontal range of about 20 km before intersecting the SOFAR channel (Chaplin, 1990). Therefore, intermediate transponders moored at the depth of the deep sound channel, are required to relay the telemetered signals from the IESs to the base station. Figure 4 shows a diagram of the moorings for the intermediate transponders. A transponder, sitting in the SOFAR channel, capable of receiving 10-kHz signals and then retransmitting, after frequency down-shifting for more efficient horizontal transmission, can service several IESs within a radial distance of 20 km.

The telemetry IES sites used in this deployment were situated such that one intermediate transponder could service each pair of IESs. The inset of Figure 1 shows a schematic of the actual deployment. Two types of intermediate transponders were used. There was one modified SOFAR float (hereafter denoted CT or central transponder) that directly serviced the IES at site C2 and relayed the data from all other IESs to Bermuda via 260 Hz signals. The other two intermediate transponders (hereafter denoted as OT or overhead transponders) each relayed data from two IESs to the CT at 780 Hz. The OTs were used because it was originally believed that they would be less expensive than the CTs. We have subsequently found that the cost difference is minimal. We would probably not use OTs in a future deployment but rather all CTs. The range of the 780 Hz OT to CT link is reliable to about 200 km. The actual distances between the transponders in this deployment were less than 60 km (Chaplin, 1990). At each stage of the relay system the frequency

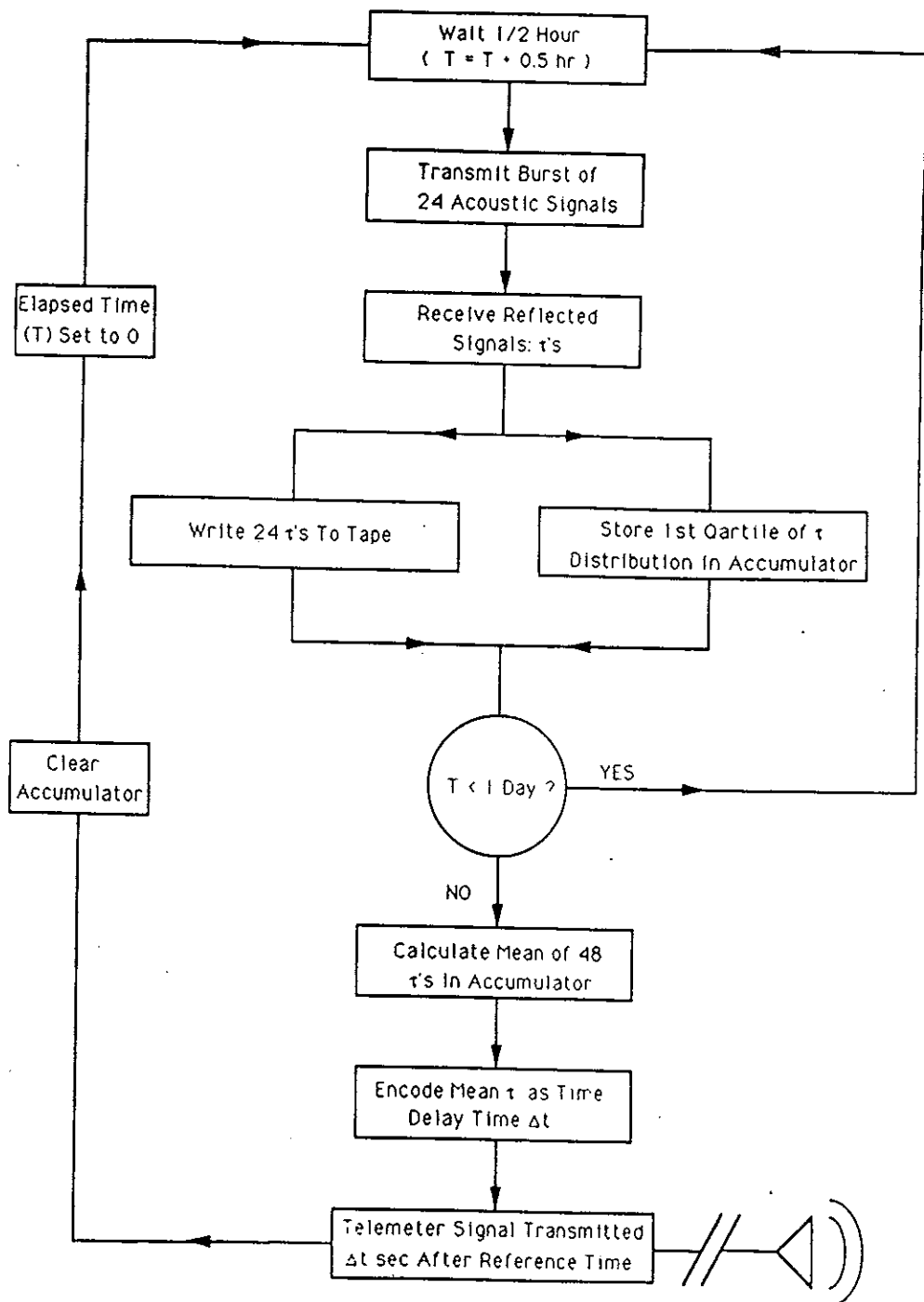


Figure 2: IES data acquisition and internal processing flow chart. In a one day cycle 1152  $\tau$ s are written to tape, 48 first-quartile points  $\tau_{1q}$  are determined, and 1  $\tau_m$  is telemetered.

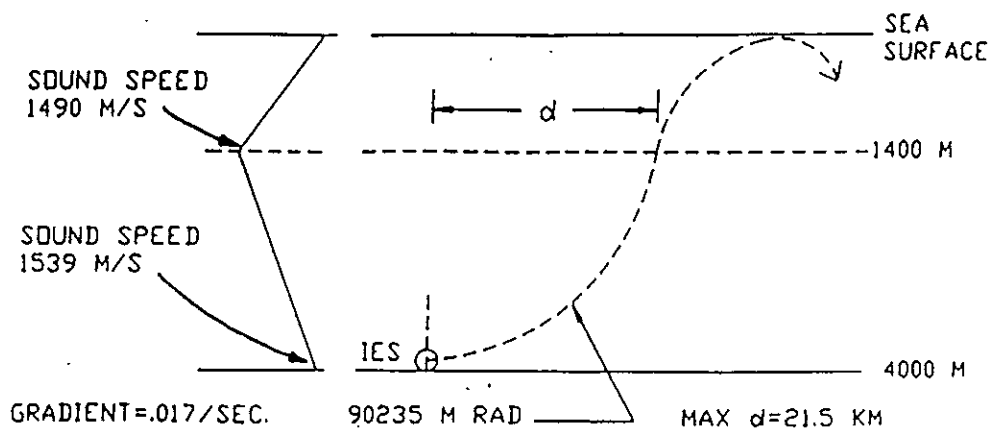


Figure 3: IES acoustic field ray diagram.

of the signal is down-shifted while preserving its time delay or, equivalently, the data information.

### 2.3 Base Station

The base station was located at the U.S. Navy Underwater Systems Center (NUSC) field station on Bermuda known as the Tudor Hill laboratory. As previously mentioned, the base station was originally established to monitor the performance of the moored SOFAR sound sources. For that purpose, occasional down time of the station was not a critical problem. The station would, at predetermined times, listen for the sound source signals and record the time of arrival. This allowed any clock drifts of the sources, and hence RAFOS float position errors, to be corrected. Since the clock drifts were essentially linear over the periods normally experienced for listening station down time, the listening gaps did not affect the quality of the RAFOS float data.

In principle, the only necessary modification to the base station for its use in the IES telemetry system would have been to increase its number of daily "listening windows" for acoustic signals. However, we made several other changes to upgrade the system. First, we added the capability to store and transmit data over modems and telephone lines back to our offices in Rhode Island. The clock that the old receiver used had a drift problem which had to be closely monitored. For this reason a completely new receiving system was installed at the station. To ensure redundancy, the existing receiving system (R0) was left intact to operate in parallel with the new one. As with the old receiver clock, the clocks of the new receivers were periodically checked against a very stable Cesium clock at the Naval lab.

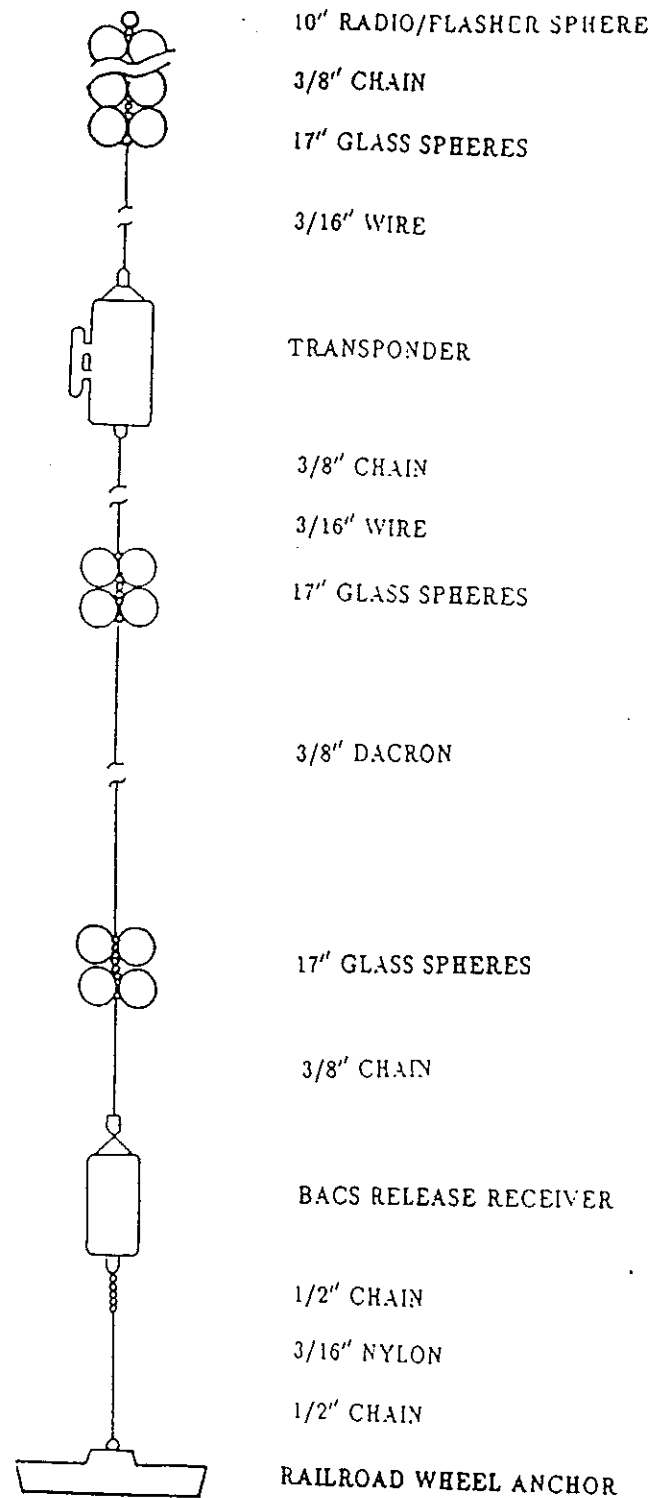


Figure 4: Schematic of Intermediate Transponder mooring.

The new system had two different receiving units, a heterodyne receiver (R1), like the original receiving system, and a homodyne receiver (R2). The homodyne receiver was installed to test its performance relative to the heterodyne receiver for possible use in future systems. For each listening period, each receiver would select the two signals most correlated with a reference signal. Unlike the old system which just recorded the arrival times of detected signals, the new receiving system automatically converted each arrival time into the time delay, in deciseconds, between the arrival time and a reference time. The time delays as well as the correlation values of the two selected signals were available in the data record. The new system had the capability to store and transmit data via modems. This made it possible to transfer the data to computers at URI at convenient intervals. The data from each receiver was also sent to a printer so that the Navy could monitor what was being sent out from the lab. Figure 5 shows a block-diagram of the receiving system on Bermuda.

## 2.4 Signal Timing

Figure 6 shows the timing of the telemetered signal as it is relayed from an IES to Bermuda.  $\Delta T$  is the 0-8.5 min-delay-encoded signal, of 50 ms duration, transmitted by the IES. After detecting the signal, the OT retransmits the signal to the CT.  $\Delta T_{OC}$ , the delay time between transmission from the OT until reception at the CT, and  $\Delta T_{CS}$ , the delay time between transmission from the CT and reception at Bermuda, are nearly constant because they are primarily related to the distance separating the sites. The time of arrival of the signal at Bermuda is linearly related to  $\Delta T$ . Tom Rossby (personal communication) had found earlier that the scatter in arrival times of a SOFAR sound source moored south of Cape Hatteras was approximately 2 s. This is the nominal scatter we expected for "good" signals received at Bermuda.

The multiple signals from both the IES telemetry system and the RAFOS navigation sound sources followed a fixed transmission schedule so that there was no interference between them at the listening station on Bermuda. The schedule for IES telemetry transmission, OT and CT listening/transmission, RAFOS navigation transmission, and base station listening is shown in Figure 7.

## 3 Chronology

A brief chronology of the telemetry deployment is shown in Table 2. Note that the telemetry signals from the original IES at site C2 were interfering with those from sites B2 and B5. Thus, telemetered data from the IESs at sites B2 and B5 were not received until after the IES at site C2 was changed. The resulting ~50 day gaps at the beginning of the telemetry records for IESs B2 and B5 are seen in Figure 15.

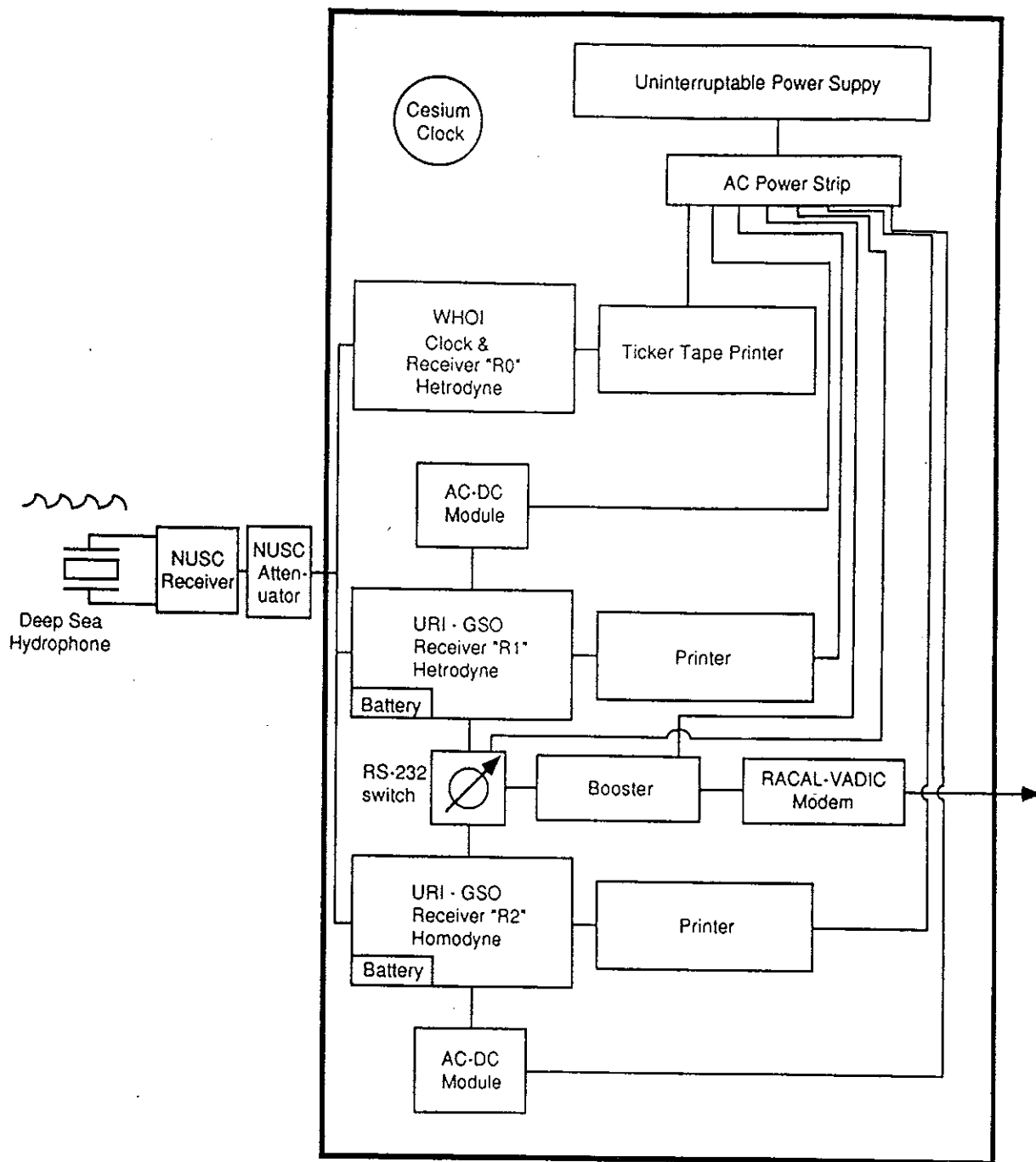


Figure 5: Block Diagram of Base Station on Bermuda. The homodyne receiver was evaluated for possible use with the RAFOS floats. It proved to be as effective as the hetrodyne receiver. Note that the modem could only be connected to one receiver at a time.

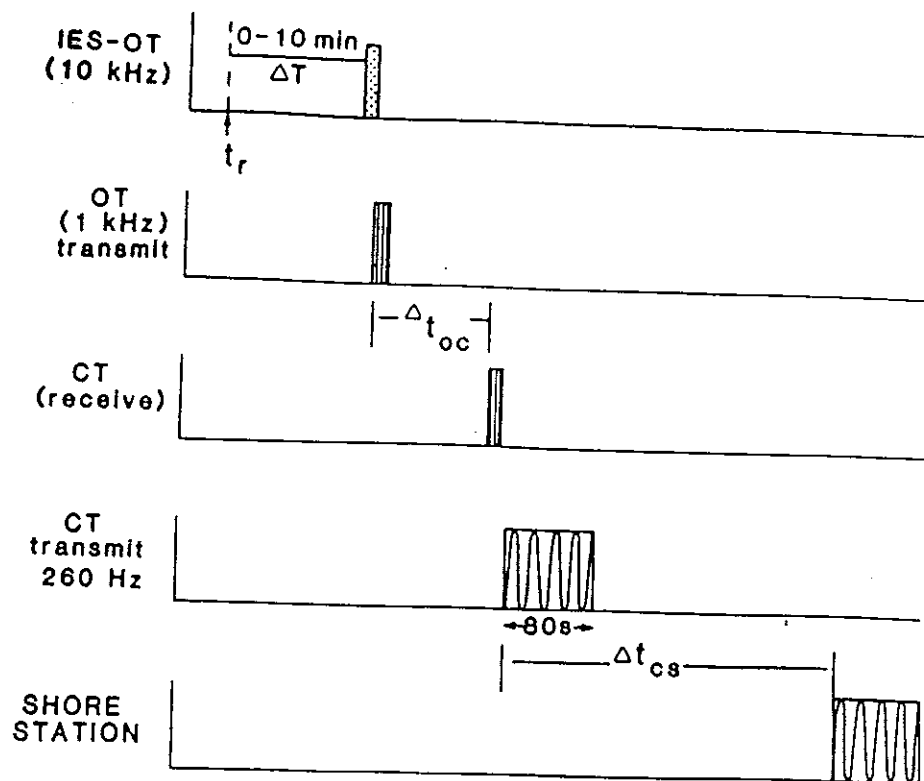


Figure 6: The timing of the delay encoded telemetered signal as it is relayed from an IES to Bermuda.

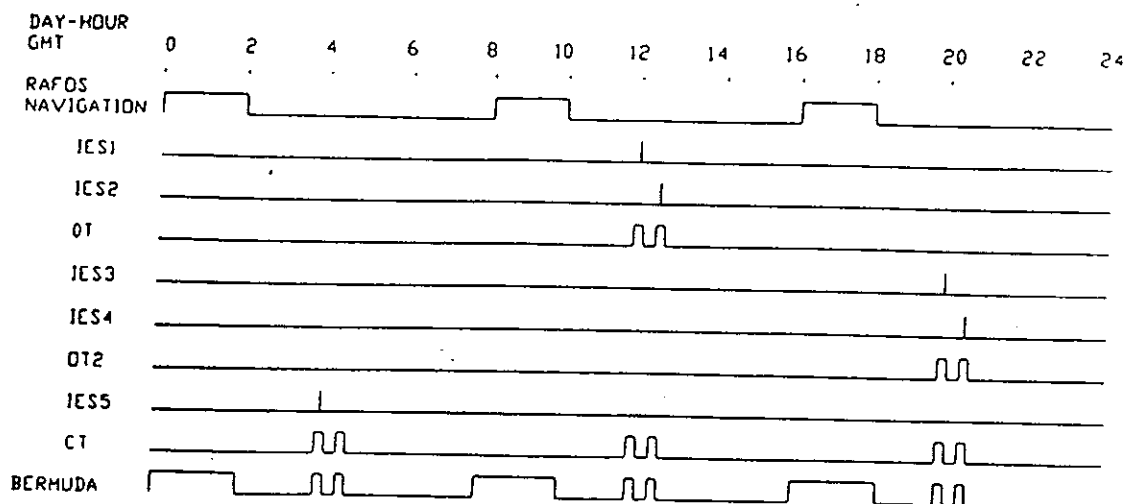


Figure 7: Schedule for telemetry system and RAFOS navigation reception/transmission.

Table 2: Chronology of the Telemetry Deployment

Date	Yearday	Comment
Aug 10, 1989	222	The receiver (R1) was installed on Bermuda by Skip Carter. The old receiver (R0), which was connected to the ticker-tape printer was accidentally unplugged.
Mid. Aug Aug ?		IESs, modified to telemeter their data to Bermuda, were deployed.
Oct 3, 1989	276-277	Old Ce clock failed sometime in August.
Oct 16, 1989	289	Receiver R0 reattached and reset
Oct 17, 1989	290	New Ce clock installed
Nov 30, 1989	334	Replaced IES C2 (Gerry Chaplin on Cape Henlopen). Started receiving from IESs B2 and B5.
Jan 15-16, 1990	15-16	Jim Fontaine resets the Bermuda Ce clock and all of the other clocks. Reset clock in receiver R1 (Chaplin tests the homodyne and heterodyne (receivers).
Aug-Sept 1990		Telemetry IESs pulled out of water.

#### 4 Data Representation: Telemetered And Taped

In this section an overview is given of the steps in the evolution of an IES internal data word into a data word written to tape and a telemetered data word. In the former case the internal data word represents an "instantaneous"  $\tau$ , while in the latter case it represents a daily average  $\bar{\tau}$  (See Section 2.1). In order to lay the ground work for subsequent sections, which will include data processing descriptions and comparisons between taped and telemetered data, the conversion of both types of datawords into thermocline depth will also be described.

The IES internal clock is nominally set to 20480 Hz. Each count (IESCT) of its data word is then equivalent to  $20480^{-1}$  s which is the time resolution of the instrument.

For an IES deployed at 5000 m depth, the travel time measurement is nominally 6.9 s or 141241 IESCTs. In general, 18 bits are required to store the full data word. However, the data word written to tape is the IES data word truncated to the 13 least significant bits (LSB). This effectively subtracts off a common amount of time from the measured  $\tau_s$ , which is due to the depth of the instrument not to changes in the average temperature of the water column. The conversion between IESCTs and the data written to tape ( $NCTs$ ) is

$$IESCT = NCT + NCT_0 \quad (1)$$

and the conversion between  $\tau$  and  $NCT$  is

$$\tau = \frac{NCT + NCT_0}{20480Hz} \quad (2)$$

where,  $NCT_0$  represents a standard amount of time for each IES which is subtracted off by truncating the data word. The time

$$\tau' = \frac{NCT}{20480Hz} \quad (3)$$

can be thought of as a travel time anomaly.

The travel time  $\tau$ , measured by the IES, is linearly related to the depth of the main thermocline, which we define as the depth of the 12°C isotherm ( $Z_{12}$ ). The relationship

$$Z_{12} = m \cdot \frac{NCT + NCT_0}{20480 \text{ Hz}} + B \quad (4)$$

can be written

$$Z_{12} = m \cdot \frac{NCT}{20480 \text{ Hz}} + B' \quad (5)$$

where

$$B' = B + m \cdot \frac{NCT_0}{20480 \text{ Hz}}. \quad (6)$$

Thus, when calibrating an IES using  $\tau'$  a different intercept is calculated than if the original data word  $\tau$  was available. However, both calibrations give identical  $Z_{12}$ , so it is not necessary to keep track of the constant  $NCT_0$ .

The telemetered data word manipulation and subsequent encoding is somewhat more involved, but it is still straightforward. Before encoding the travel time into a delay time, the IES truncates the data word from the full 18 bits to the middle 8 bits, keeping only bits 4-11 (See Figure 8). Thus, not only is a common time subtracted off of each  $\tau$  by throwing out the 7 most significant bits (MSB), but each count ( $TELCT$ ) of the new data word is equal to eight of the original counts since the 3 LSBs are thrown out. The data word manipulation is schematically shown in Figure 8. The conversion between  $TELCT$ s and  $IESCT$ s is then

$$IESCT = 8 \cdot TELCT + IESCT_0, \quad (7)$$

where  $IESCT_0$  is a constant number of counts subtracted off by truncating the 7 MSBs.

The IES constructs a time delay ( $\Delta t$ ) which is equal to  $TELCT \cdot 2$  s, i.e., with a granularity of 2 s. Thus, 2 s of delay is allowed for each 8 counts of the original data word. It is important to note, however, that this conversion is only accurate to 7  $IESCT$ s because of the truncation of the least significant bits of the original data word. The resolution of  $\tau$  has been reduced from  $(20480 \text{ Hz})^{-1}$  to  $8 \cdot (20480 \text{ Hz})^{-1}$  because of the truncation of the 3 LSBs from the original data word. Equivalently, the resolution has been reduced from 1.0 m to 7.8 m of  $Z_{12}$  (the slope  $m$  in the above equation has been found to be  $-19840 \text{ m s}^{-1}$ ).

At Bermuda, the signal is measured in deci-seconds of delay time of the received signal. That is, each count of the data word ( $BDACT$ ) is equal to 1 deci-second of delay time. The conversion between  $BDACT$  (received delay time) at Bermuda and  $TELCT$ s is

$$TELCT = \frac{1 \text{ ds} \cdot (BDACT + BDACT_0)}{10 \text{ ds s}^{-1} \cdot 2 \text{ s}} \quad (8)$$

where  $BDACT_0$  is a fixed positive or negative quantity representing delay time offset which arises because the reference time on Bermuda, for the telemetered signal, is not exactly equal to the sum of the reference time at the IES and the signal transit time from the IES to Bermuda.

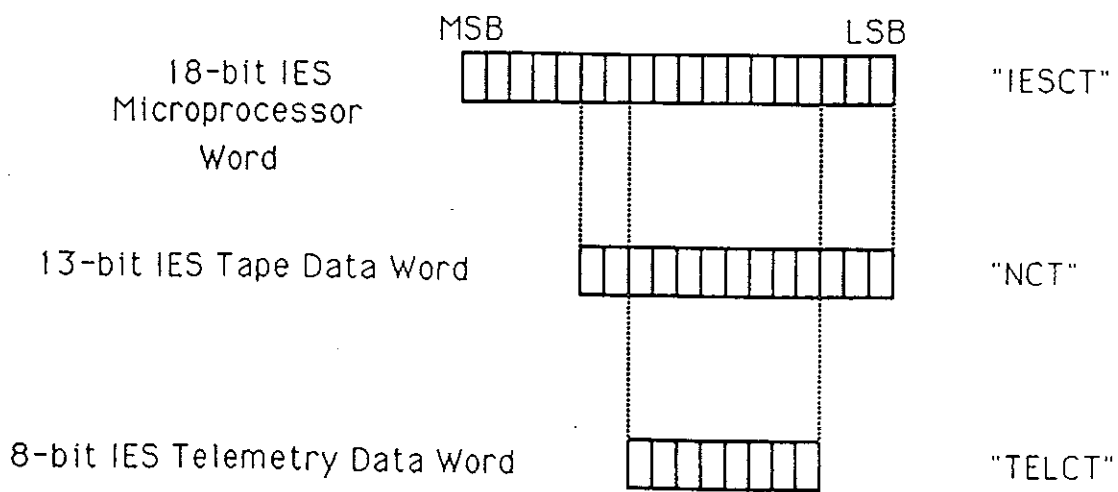


Figure 8: All of the IES internal processing is done with 18-bit words. The data word is truncated to the 13 least significant bits before being written to tape. Before being encoded as a time delayed telemetered signal the data word is truncated to bits 4-11.

Table 3: The conversions between  $\tau$ , the counts written to the IES tape ( $NCT$ ) and the counts measured at Bermuda ( $BDACT$ ).  $N_0$  is a constant for each IES and is introduced by any travel time between the IES and Bermuda of the telemetered signal which is not accounted for in the time delay introduced between when the signal is sent from the IES and when the Bermuda receiving station begins to "listen".

$\tau$ (s) $10^{-3}$	NCT	Delay Time (s)	BDACT (ds)
2	4	0.5	$5 + N_0$
25	512	64	$640 + N_0$
50	1024	128	$1280 + N_0$

In a manner similar to equation 5 for the data written to tape,  $Z_{12}$  can be related to  $BDACTs$  through the relation

$$Z_{12} = m \cdot C \cdot BDACT + B^\dagger \quad (9)$$

where  $C$  is the conversion factor between  $BDACTs$  and travel time of the IES measuring signal, and  $B^\dagger$  is the modified intercept which has absorbed both the truncation of the MSBs and constant delay time offsets ( $BDACT_0$ ). The conversion factor  $C$ , is given by

$$C = \frac{1ds \cdot 8}{10dss^{-1} \cdot 2s \cdot 20480Hz}, \quad (10)$$

or

$$C = \frac{1s}{51200}. \quad (11)$$

Note that  $C$  for the tape data is  $(20480 \text{ Hz})^{-1}$ .

Table 3 lists the IES data written to tape and telemetered data for a few sample  $\tau$  values.

## 5 Processing

This section describes the processing for the telemetered and taped data. Flow charts of the processing steps for taped and telemetered data is shown are Figure 9. These charts assume that the IESs have been calibrated, and in the case of the telemetered data, that they have been de-drifted. The details of the processing steps are described in the following subsections. Note that the taped data consists of the "traditional" data (a burst of 24  $\tau$ s every 1/2 h) and data used for telemetry (the representative  $\tau$  ( $\tau_{1q}$ ) calculated by the IES for each burst).

### 5.1 Taped Data

The processing of the taped data is fully described in Fields, et. al., (1991), so the description here will be brief. As described in Section 2.1, every half hour an IES emits a burst of 24 acoustic measuring signals. The IES writes all 24  $\tau$ s to tape along with a time which corresponds to the first quartile point in the distribution of the 24  $\tau$ s. The first 24 data words ( $\tau$ s) are used in the

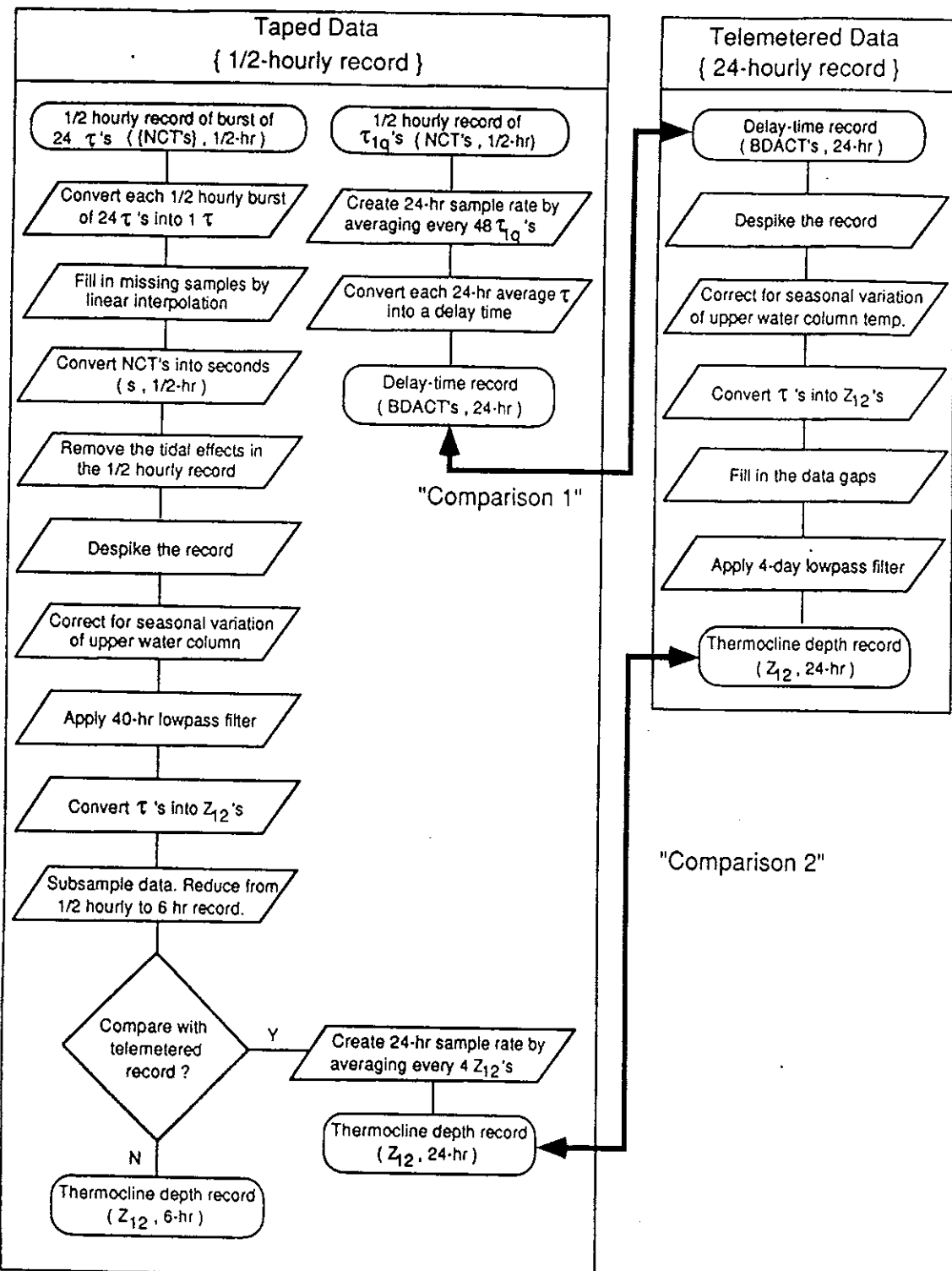


Figure 9: The flow charts showing the basic processing of the taped and telemetered data are shown on the left and right panels respectively. Also indicated are the types of comparisons made between the taped and telemetered data.

traditional processing of the IES taped data and the 25th data word ( $\tau_{12}$ ) is used exclusively for reconstructing the data telemetered from the IES.

### 5.1.1 Calibration of $\tau$ to $Z_{12}$

The taped records are converted into  $Z_{12}$  records using Equation 5. The factor  $m$  in the equation is known in the Gulf Stream region (see Howden, et. al.,(1992)), and  $B'$  (or  $B_{int,tape}$ ) is determined individually for each IES. The calibration curve for each IES is determined once its  $B_{int,tape}$  is found. The following are the steps for finding  $B_{int,tape}$  for each IES. During deployment and recovery cruises, a total of  $N_i$  XBT casts are taken at the  $i$ th IES site. The temperature profile of each XBT cast is integrated from 250 m to 750 m yielding a quantity  $Q$  ( $Q = \int_{250m}^{750m} T dz$ ). The quantity  $Z_{12}^*$  is calculated from an empirical functional fit of  $Z_{12}$  to  $Q$  from over 6,000 XBT casts (from NODC archives) taken in the Gulf Stream region. The  $N_i Z_{12}^*$  values are substituted into Equation 5 along with the  $N_i$  coincident  $\tau$  measurements from the recovered data tape, yielding  $N_i$  values of  $B_{int,tape}$ . The  $B_{int,tape}$  used in the calibration curve is the average of the  $N_i B_{int,tape}$ s.

The motivation of using  $Z_{12}^*$ , rather than  $Z_{12}$ , in the calibration process is that it eliminates the high frequency noise that can be present when a point measurement ( $Z_{12}$ ) is made of the thermocline depth. Hereafter  $Z_{12}^*$  will be simply denoted as  $Z_{12}$ , it being understood that in the calibration process  $Z_{12}$  refers to the calculated value  $Z_{12}^*$ .

### 5.1.2 Traditional Processing of Taped IES Data

After an IES has been recovered and its data tape read into a computer, a number of preliminary steps are taken to obtain a record of  $\tau$  versus time (see Fields, et., al., (1991)). For this discussion, the important step is the fit of each half-hourly set of 24  $\tau$ s to a Rayleigh distribution. The mode of each distribution is taken to be  $\tau$  for that particular sample. Unlike the telemetered data record which is composed of daily averaged  $\tau$ s, the taped record has a half-hourly sample rate and has to be corrected for changes in travel time due to the tides. Next, the taped record is passed through a program which removes outliers and replaces them with linearly interpolated values. The "cleaned up" data is then corrected for changes in the travel time due to the seasonal variation of the temperature of the upper water column. A low-pass 2nd order Butterworth filter, with a 2-d cutoff period, is then applied forwards and backwards to the data to remove high frequency fluctuations. The record is then subsampled, reducing it from a 1/2 hour sample rate to a 6 hr sample rate. Finally, the  $\tau$  record is converted to a  $Z_{12}$  record using Equation 5 and the Bints in the third column of Table 4.

For comparison with the ( $Z_{12}$ , 24-hr) telemetered record (*Comparison 2*), the fully processed ( $Z_{12}$ , 6-hr) record is converted to a 24-hr sample rate by averaging every 4  $Z_{12}$ s. This, of course, is not part of the traditional processing but is simply done for the comparison.

### 5.1.3 Reconstruction of the Telemetered Data

As described in Section 2.1, the 25th data word of each taped record is the representative travel time ( $\tau_{1q}$ ) of the burst of 24  $\tau$ s in the record chosen by the IES. Internally, the IES averages every 48 of the these data words and calculates a delay time proportional to the averaged value. To convert the 1/2-hourly record of  $\tau_{1q}$ s into the information that was telemetered from the IES, the following steps are done. First, every 48  $\tau_{1q}$ s are averaged to produce a 24-hr sample rate ( $\overline{\tau_{1q}}$ , 24-hr). The  $\overline{\tau_{1q}}$  are then converted from *NCT*s into *TELCT*s by dividing by 8, since each *TELCT* equals 8 *NCT*s. Next a delay time is calculated using

$$\Delta T = \overline{\tau_{1q}} * 20ds \quad (12)$$

The resulting record ( $\Delta T$ , 24-hr) can then be directly compared with the delay times as measured at Bermuda (*Comparison 1*).

## 5.2 Telemetered Data

The basic processing of the telemetered data is done in the 6 steps that are described in the following subsections. Figures 10 to 13 show the raw data and the results of each processing step that give a visually distinct change between the input and output.

### 5.2.1 IES Clock-Drift Correction

Because of inaccuracies in the setting of the IES clock frequencies, the telemetry records had to be de-drifted. The clocks used in the IESs are accurate to  $0.01 \text{ s d}^{-1}$ . A drift rate of this magnitude was deemed small enough to yield thermocline depth estimates within our stated accuracy of 20 m. For example, a drift rate of  $0.01 \text{ ds d}^{-1}$  would yield a maximum clock drift of 3.65 s over the one year deployment of the instruments which in turn would translate into an apparent drift of  $Z_{12}$  of 14 m. Although the IES  $\tau$  measurement has a resolution of 1 m, the accuracy of an IES calibration into  $Z_{12}$  is only 20 m because of the uncertainty of the intercept ( $B_{\text{int}}$ ) of the linear relation between  $Z_{12}$  and  $\tau$ . Since the calibration uncertainty is greater than the error introduced by an actual frequency drift of the IES clocks, we elected to simplify the telemetry design by excluding a method to check for clock drifts. Unfortunately, we discovered after the experiment was underway that the instrument used to set the IES clock frequencies was not accurately calibrated. Thus the clock timing effectively drifted at a much higher rate than anticipated. While these clock drifts do not significantly affect the actual travel times measured by the IESs, they do contaminate the telemetered data. The basic information of the telemetry system is in the arrival time of the signal *relative* to a fixed reference time. Large clock drifts would then shift the arrival times, which would in turn be falsely interpreted as a change in  $Z_{12}$ .

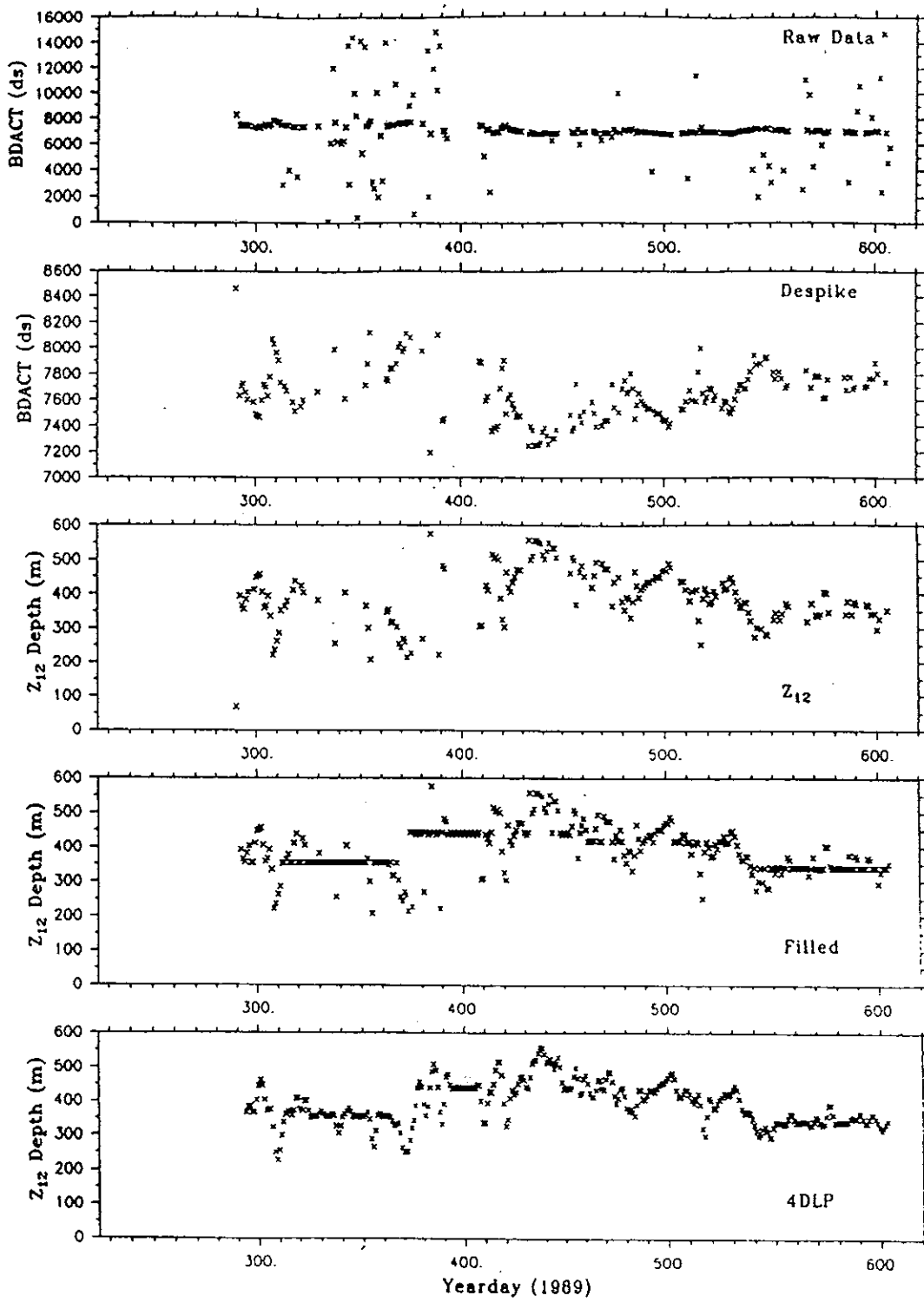


Figure 10: The top panel shows the *BDACT* as measured at Bermuda for the IES at site B2. Successive panels show the output of the processing steps which are visually distinct.

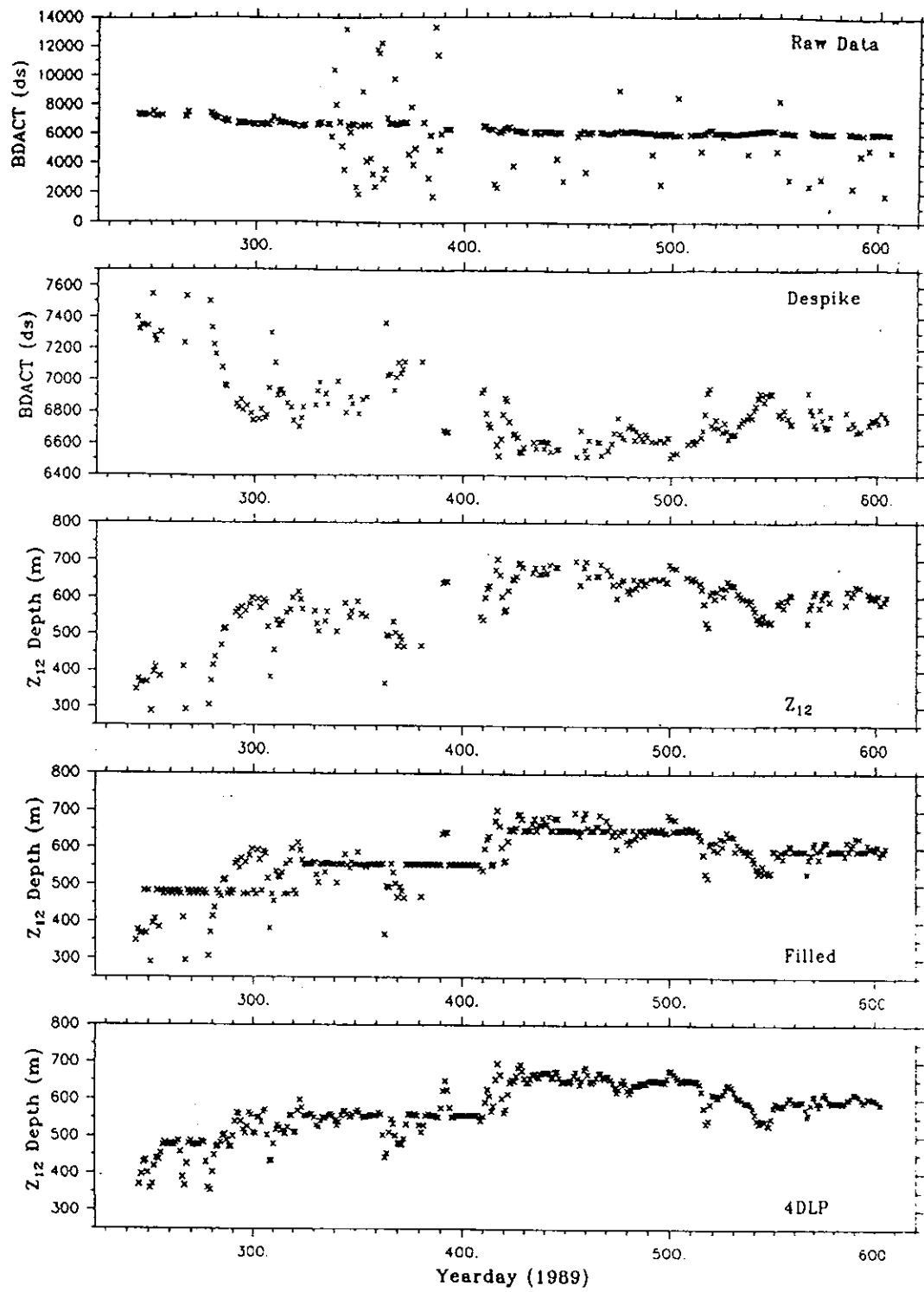


Figure 11: The top panel shows the *BDACT* as measured at Bermuda for the IES at site B3. Successive panels show the output of the processing steps which are visually distinct.

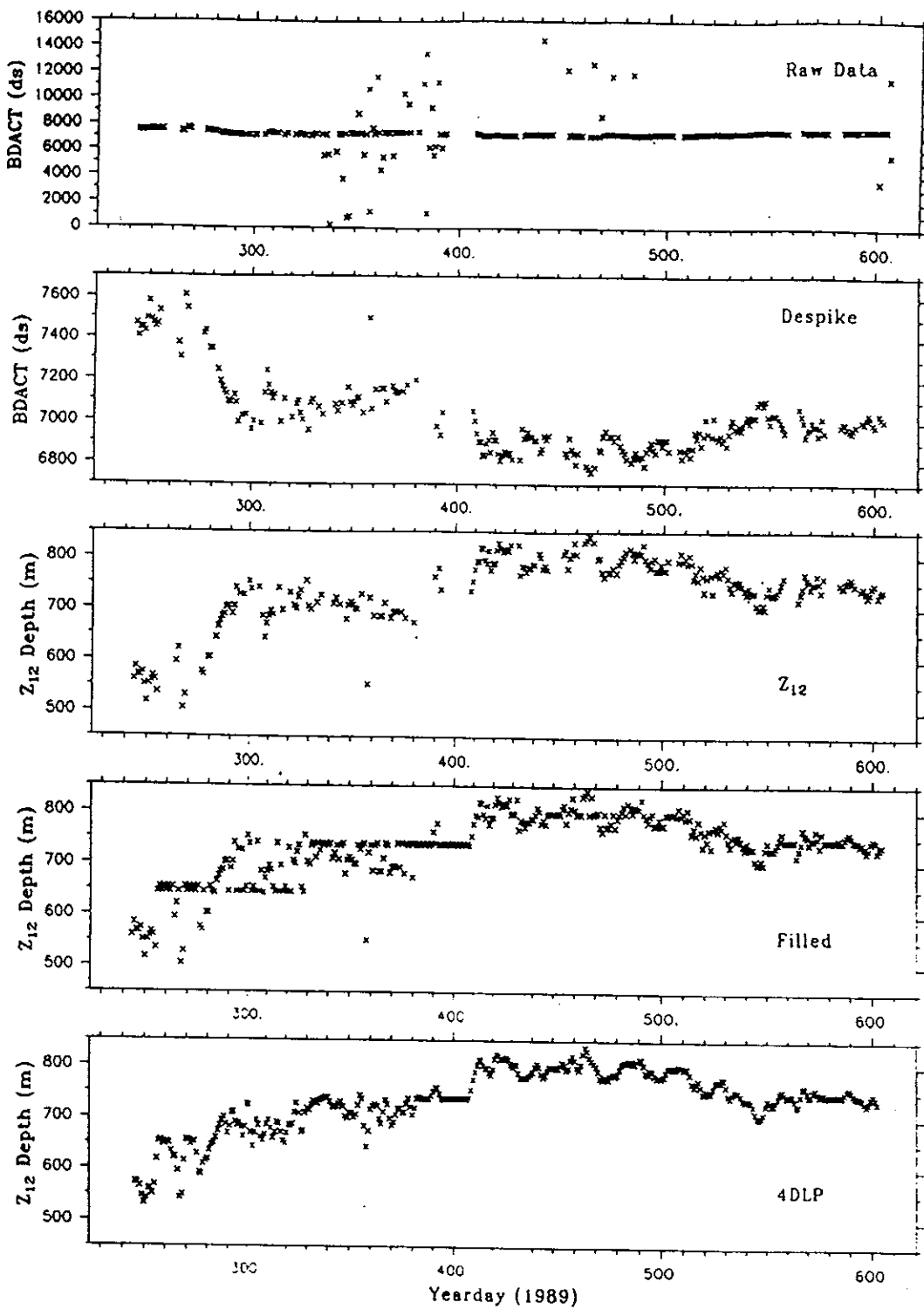


Figure 12: The top panel shows the *BDACT* as measured at Bermuda for the IES at site B4. Successive panels show the output of the processing steps which are visually distinct.

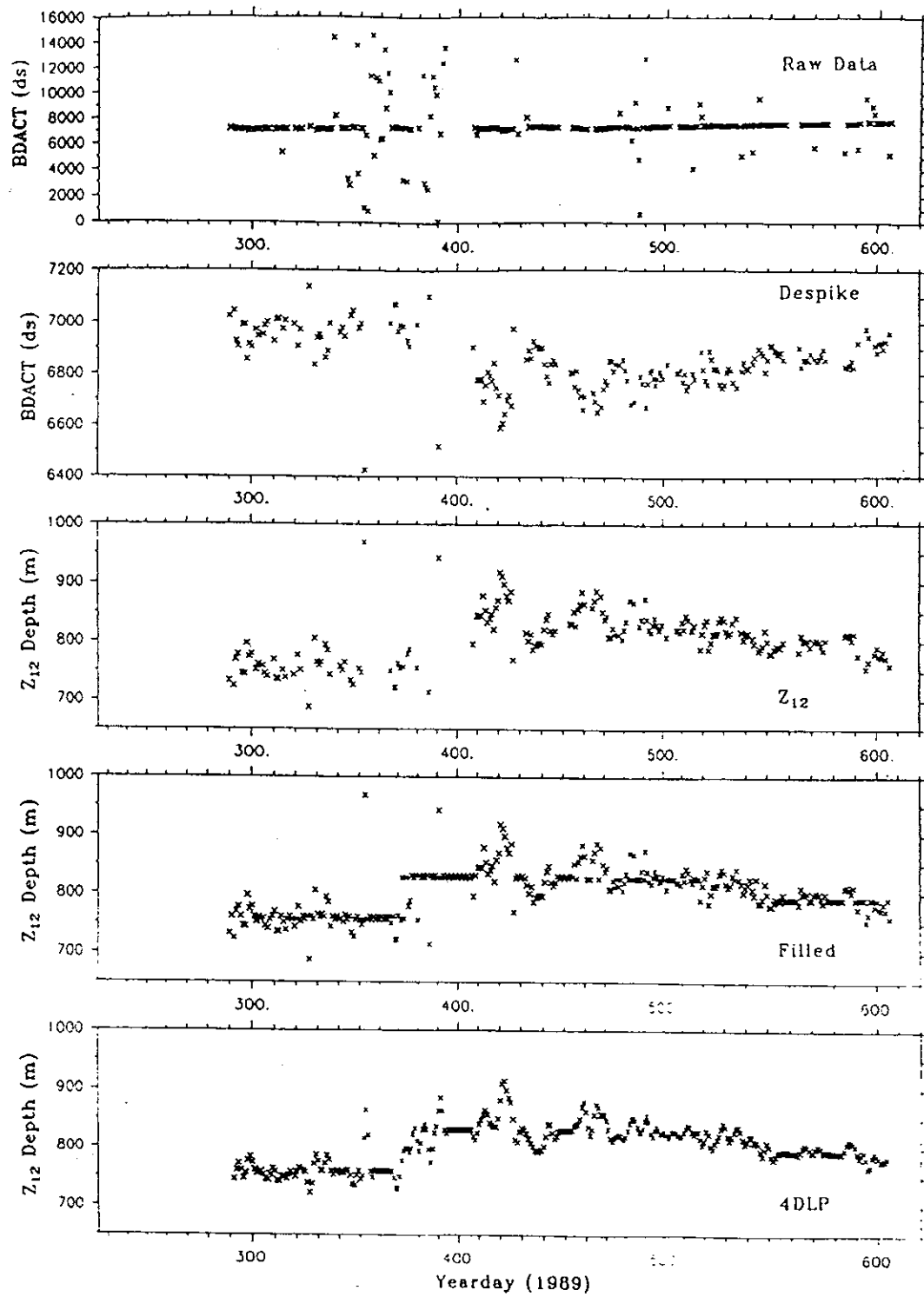


Figure 13: The top panel shows the *BDACT* as measured at Bermuda for the IES at site B5. Successive panels show the output of the processing steps which are visually distinct.

While the IESs were still moored at sea, the frequency counter was recalibrated and crude estimates of the clock drifts were made. This allowed us to make preliminary corrections to the telemetered data while the system was still operational. However, more accurate drift corrections could not be performed until the IESs were recovered. The drift rate was calculated individually for each IES as the slope of the best straight line fit to the difference between the tape records and telemetered data records after outliers had been windowed out. An example of this process is shown in Figure 14 for IES B3. Since IES B2 was not recovered we were unable to use this technique at that site. Instead, we simulated the B2 tape data by averaging the B1 and B3 tape records. Then we compared the simulated data with the actual telemetered B2 data to obtain the drift rate of the clock.

### 5.2.2 Calibration of $\tau$ to $Z_{12}$

In principle, the Bints for the telemetered data  $Bint_{tel}$  are calculated identically to those for the tape records: the  $Z_{12}$  obtained from XBT casts at the IES sites are compared with the coincident delay times (encoded  $\tau$ ) received at Bermuda. However, the telemetry system was not operational when the IESs were first deployed and the XBT casts taken. Thus a crude calibration was initially done using the XBT casts taken at deployment and the first telemetered  $\tau$ s received at Bermuda several days after deployment. Subsequently, after the IESs were recovered, we were able to perform better calibrations by using the taped data which were calibrated with coincident XBT casts taken during both the deployment and recovery cruises. The Bints for the de-drifted telemetry records were calculated in this manner as

$$Bint_{tel} = -19840ms^{-1} \cdot \frac{(BDACT_{tape} - BDACT_{tel})}{51200dss^{-1}} + Bint_{tape}, \quad (13)$$

where  $BDACT_{tel}$  are the data words of the received telemetered data and  $BDACT_{tape}$  are the converted taped data words.

The drift rates are shown in Table 4, along with the Bints for both the telemetry data records and the tape data. The table shows two entries for the telemetry Bints. The first entry, the direct method, is the Bint calculated from Equation 9 using the  $Z_{12}$ s of the XBT casts taken during recovery and deployment and the first and last  $\tau$ s from the telemetry records. Because the XBT casts and  $\tau$ s were separated by as much as several days, this calibration is not as accurate as that for the taped data for which coincident XBT casts and  $\tau$ s are available. At deployment this method must be used to obtain an initial calibration using the XBT casts taken at that time. In a future deployment, it would be desirable to have the telemetry system operational so that the initial calibration could be done with coincident (i.e., within one day) XBT casts and telemetered  $\tau$ s. As discussed in Section 3, the telemetered signals for IESs B2 and B5 were blocked by the signals from the original IES at site C2 for the first ~46 days of deployment. The initial calibrations for IESs B2 and B5 were inferred

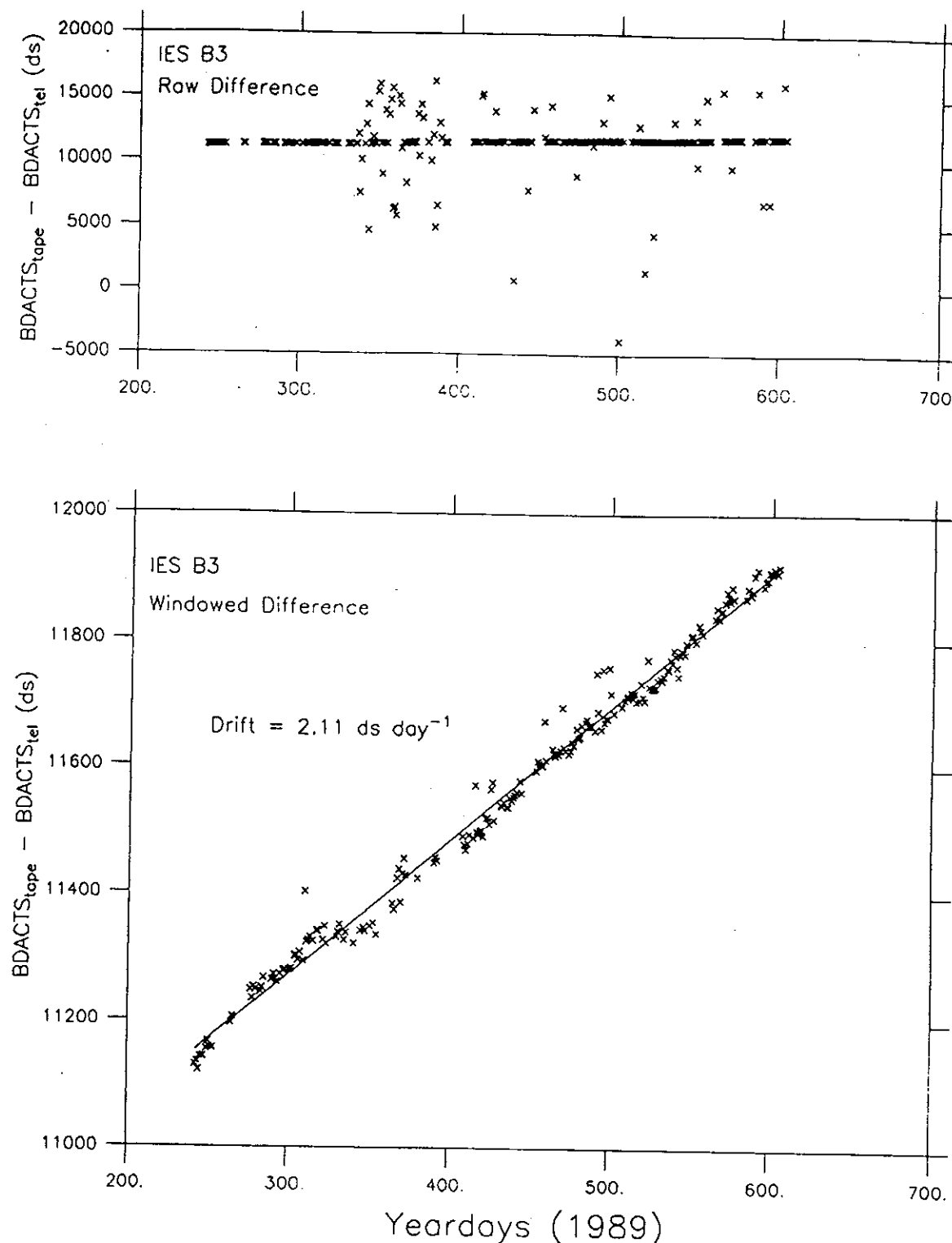


Figure 14: The top panel shows the difference between the taped record, converted to  $BDACT_s$  and the telemetered record for IES B3. The bottom panel shows the windowed difference record with a superimposed least squares straight line fit. The slope of the line gives the drift rate of the instrument.

from the initial calibrations of IESs B3 and B4 using the following method. At deployment,  $Z_{12}$  was known at sites B2 and B5 from XBT casts taken at that time. Although coincident  $\tau$ s were not telemetered from these two IESs, relatively coincident (i.e., within several days)  $\tau$ s were telemetered from adjacent IESs (B3 and B4). Once the IESs at sites B2 and B5 began telemetering their data, the average and the  $\tau$ s from the adjacent IESs were computed. These differences were added to the coincident  $\tau$ s from the adjacent sites to obtain estimated coincident  $\tau$ s from the IESs at sites B2 and B5.

The second column in Table 4 contains the Bints calculated by comparing the telemetry record and the calibrated tape record as shown in Equation 13. There is no entry for the Bint calculated by the comparison method for IES B2 since the instrument was not recovered.

Table 4: BINTs and drift rates. Columns 2 and 3 show the BINTs for the telemetered data calculated by two different methods. The first method uses the coincident  $\tau$ s, from the IESs, and  $Z_{12}$  from XBT casts. The second method uses the BINTS calculated for the taped data. Coincident pairs of  $\tau$  and  $Z_{12}$  did not exist for the telemetered data of IESs B2 and B5. Thus, the BINTS in column 2 for IESs B2 and B5 are estimated using the method described in the text. IES B2 was never recovered so there are no entries in columns 3 and 4 for it. Column 4 shows the BINTs calculated for the data put to tape. The Bints labeled with a † indicate that their calculation by the "direct method" used inferred  $\tau$ s. See the text for explanation.

IES	BINT 1	BINT 2	Drift Rate ds/day	
	Direct (m)	Comparison (m)		
B2	3367†	N/A	N/A	+2.16
B3	3162	3229	7533	+2.11
B4	3457	3469	1794	-1.30
B5	3466†	3472	1808	-2.19

### 5.2.3 Despike

The despike program removes "bad" data values if they fail either of two criteria. In the first test, data values which fall outside some specified upper and lower limits are "windowed out" as "bad" values. The range of the "good data" window differed slightly for each IES dependent upon the average location of the IES relative to the Gulf Stream North Wall. For the four IESs, the windowing range averaged 1145 ds (corresponds to 444 m main thermocline depth). In the second test, data which differ from a local mean (10 day running average) by more than a specified amount is labeled as a "bad" value. The maximum acceptable change of  $\tau$  with respect to the local mean was set at 250 ds which corresponds to a change in  $Z_{12}$  of 97 m.

#### 5.2.4 Seacor (Seasonal Thermocline Correction)

The program SEACOR corrects the  $\tau$ s for variations due to changes in sound speed in the top 200 m of the water column as the seasonal thermocline warms and cools. The seasonal correction is fully described in Fields et. al., (1991). Briefly, however, the  $\tau$ s are corrected using a long-term mean curve of travel time versus season calculated from over 12,000 XBT casts (obtained from the NODC archives) in the geographic region of the IES deployments. The correction is important since the seasonal variation of  $\tau$  in the SYNOP array region was determined to be roughly 1–1.8 ms peak to peak which corresponds to an apparent 20–36 m peak to peak variation in  $Z_{12}$ .

#### 5.2.5 $Z_{12}$

The  $Z_{12}$  program converts the BDACT directly into  $Z_{12}$  depths using the individual Bints for each IES in Equation 9. Prior to recovery, the Bints in column 1 of Table 4 were used in the program. After recovery (and for all subsequent results shown in this paper), the more accurate Bints in column 2 for IESs B3–B5 were used.

#### 5.2.6 Fill-in

Gaps in the telemetry data records arise from 2 sources: downtime of the Bermuda receiving station and false/missed  $\tau$ s. Two different methods were tested to fill these gaps in order to obtain complete continuous time-series records. The first method was simply to linearly interpolate between the good data. The results were not very satisfactory because of the relatively large data gaps ( $\sim 15$  days) during certain periods. When the data gaps were large, the linear interpolation scheme resulted in false structure to the  $Z_{12}$  record. The second method proved a bit more effective in filling the data gaps. That method used the spectral information present in the data by least-squares fitting the data to a trigonometric series. For example, let  $n$  be the actual number of data points and  $N$  be the number of data points if there were no missing data. The number of missing data points is then  $m = N - n$ . The incremental frequency is taken to be  $(N\Delta t)^{-1}$ , where  $\Delta t$  is the sampling time. Hereafter,  $\Delta t$  will be taken to be equal to 1 day. The maximum frequency is  $N(2N\Delta t)^{-1} = 0.5$ . Letting  $h(t)$  represent the demeaned data and  $\hat{h}(t) = \sum_{i=1}^{N/2} \{A_i \cos(2\pi f_i t) + B_i \sin(2\pi f_i t)\}$ , the method minimizes  $S = \sum_{j=1}^m \{h_j - \hat{h}_j\}^2$  with respect to the  $A_i$  and  $B_i$ . Since there are missing data points, this system is underdetermined and solved by singular value decomposition (SVD) and only  $(A_i, B_i)$  values are non-zero for non-singular eigenvalues of the least-squares fit. The fitted function is then “back-transformed” to yield the time series. When large data gaps are present, the method fills them with the (local) mean value of the record. In practice, the despiked  $Z_{12}$  record for each IES was separated into four approximately equal records. Each segment was run through the fill-in program and then the segments were recombined. Gaps within each segment were filled with the

mean  $Z_{12}$  for that segment. The filled records generated by the second method are shown in the fifth panel of Figures 10—13. The plateaus result from the data gaps.

### 5.2.7 Low-pass Filter

The filled  $Z_{12}$  records for the telemetered data are low-pass filtered, with a cutoff period of four days to remove high frequency fluctuations. The filter used is a 2nd-order Butterworth filter applied forward and backwards to avoid phase shifts. Note that the taped data is low-passed filtered with a cutoff period of 2 days.

## 6 Results

### 6.1 Data Return

On average, the receiving station on Bermuda was down 25% of the time. For a given IES, the downtime is calculated as any day during which no telemetered data was recovered due to problems at the receiving station. This facility, however, was originally intended to serve as a monitoring station for the SOFAR sound sources and the downtime did not adversely effect that task. While our data return is much lower than anticipated because of the downtime, the receiving station was adequate to test the telemetry system. Figure 15 indicates the data return for each IES. This data includes that which was recovered from the hard copies printed by the ticker-tape printer.

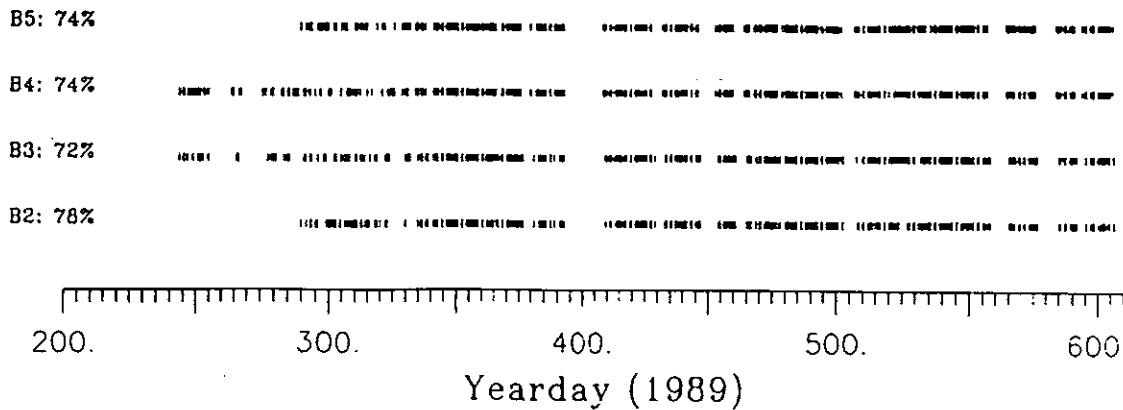


Figure 15: The days in which data was received and recorded at Bermuda and received at URI.

## 6.2 Data Acceptance

The data acceptance is defined as the amount of data which passes the despiking tests relative to the received data. The average data acceptance rate was 79%. That is, on average, 79% of the received data passed our despiking criteria involving windowing and maximum rate of change tests.

## 6.3 Delay Time Comparison

The most direct test of the telemetry system is to compare the data transmitted by the IES ("data sent") to that received on Bermuda ("data received"). The description of how the transmitted data is reconstructed from the taped data is in Section 5.1.3. The variation in the "data sent" record should ideally match the variation in the "data received" record. However, there will be an offset between the records because the transit time of the signal from an IES to Bermuda is not precisely known. Another source of offset is introduced because the taped data truncates the 5 MSBs from the original IES data word while the telemetered data word truncates the 7 MSBs. For IES B3, the offset can be seen in Figure 14 to be approximately 11150 BDACTs or 11150 ds. We can remove this offset by removing the means from the two records. Figures 16–18 show the comparisons between the transmitted and received data for sites B3, B4, and B5. No comparison was made for the IES at site B2 since the instrument was not recovered. Both the tape and the telemetered data shown in these figures have been despiked.

Listed in Table 5 are the root-mean-square (rms) differences between the tape and telemetered records, listed both directly in *BDACT* and in equivalent meters of  $Z_{12}$  depth. We used two different methods to compute these rms differences. In Method 1, the tape and telemetered data were first independently despiked and the rms differences were determined by subtracting these cleaned up records. This method gives a true measure of how well the system works in real time applications because it gives the rms difference between the two data sets when each is independently processed. In Method 2, we first subtracted the "raw" tape and telemetry data then despiked the difference record before computing the rms. This method gives values close to Tom Rossby's 20 ds scatter in arrival times of the signals from the moored SOFAR float (see Section 2.4) since the only variability not removed from the system is the scatter due to multipath ambiguities of the transmitted signal between the inlet array and Bermuda.

## 6.4 $Z_{12}$ Comparison

A comparison of the  $Z_{12}$  records for all of the telemetry IESs, with the exception of the one at site B2, is shown in Figure 19. Using only days when good data were received at Bermuda, the rms difference between  $Z_{12}$  as determined from the tape data and the telemetry data is 29 m when averaged over all of the IESs. Table 6 shows the rms values for the three individual IESs, ranging from 23–38 m. These values are higher than those shown previously in Table 5 where the average

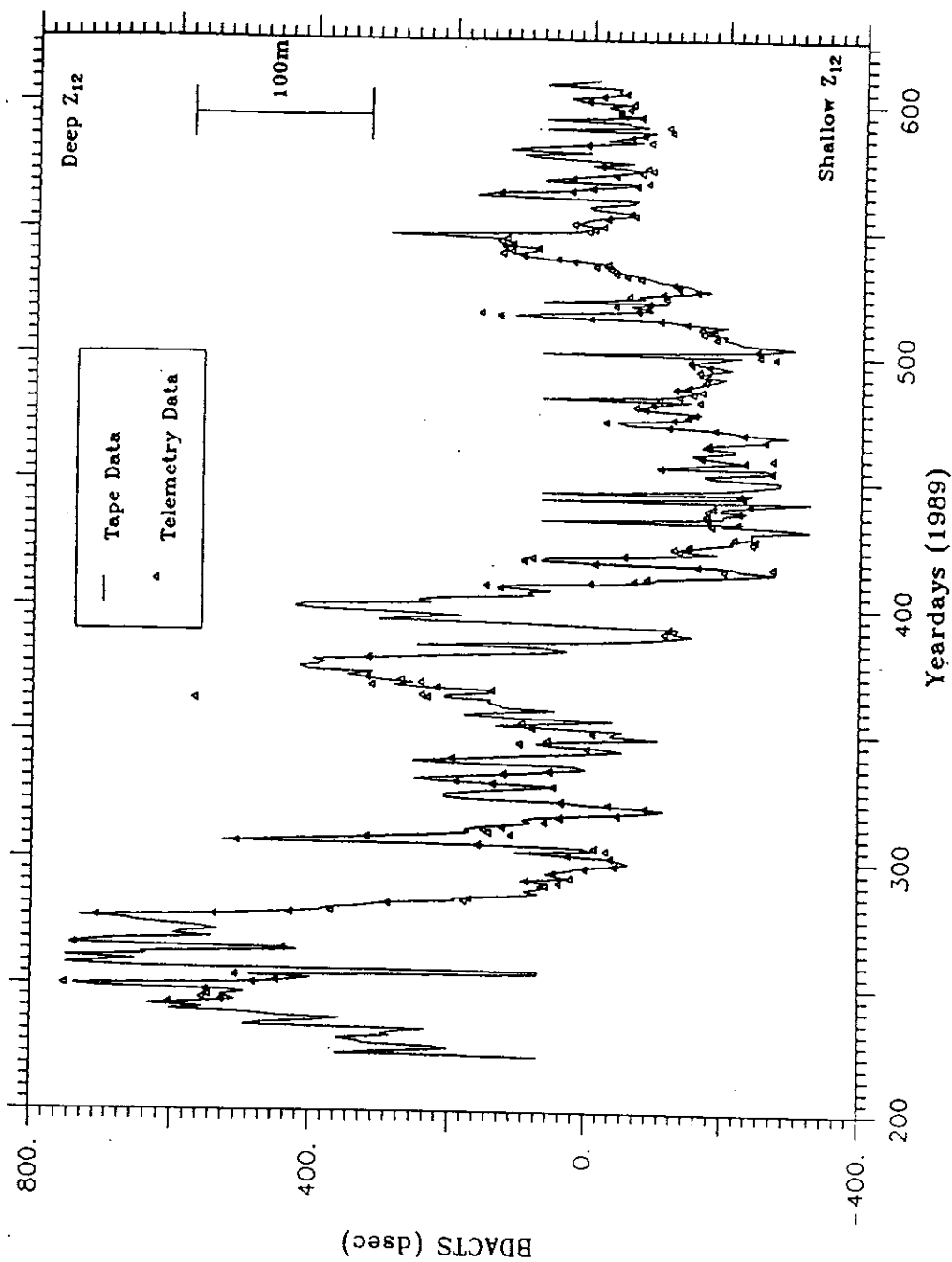


Figure 16: Comparison between the time delay as computed from the IES tape and that measured at Bermuda for IES B3. Both records have been independently despiked and demeaned.

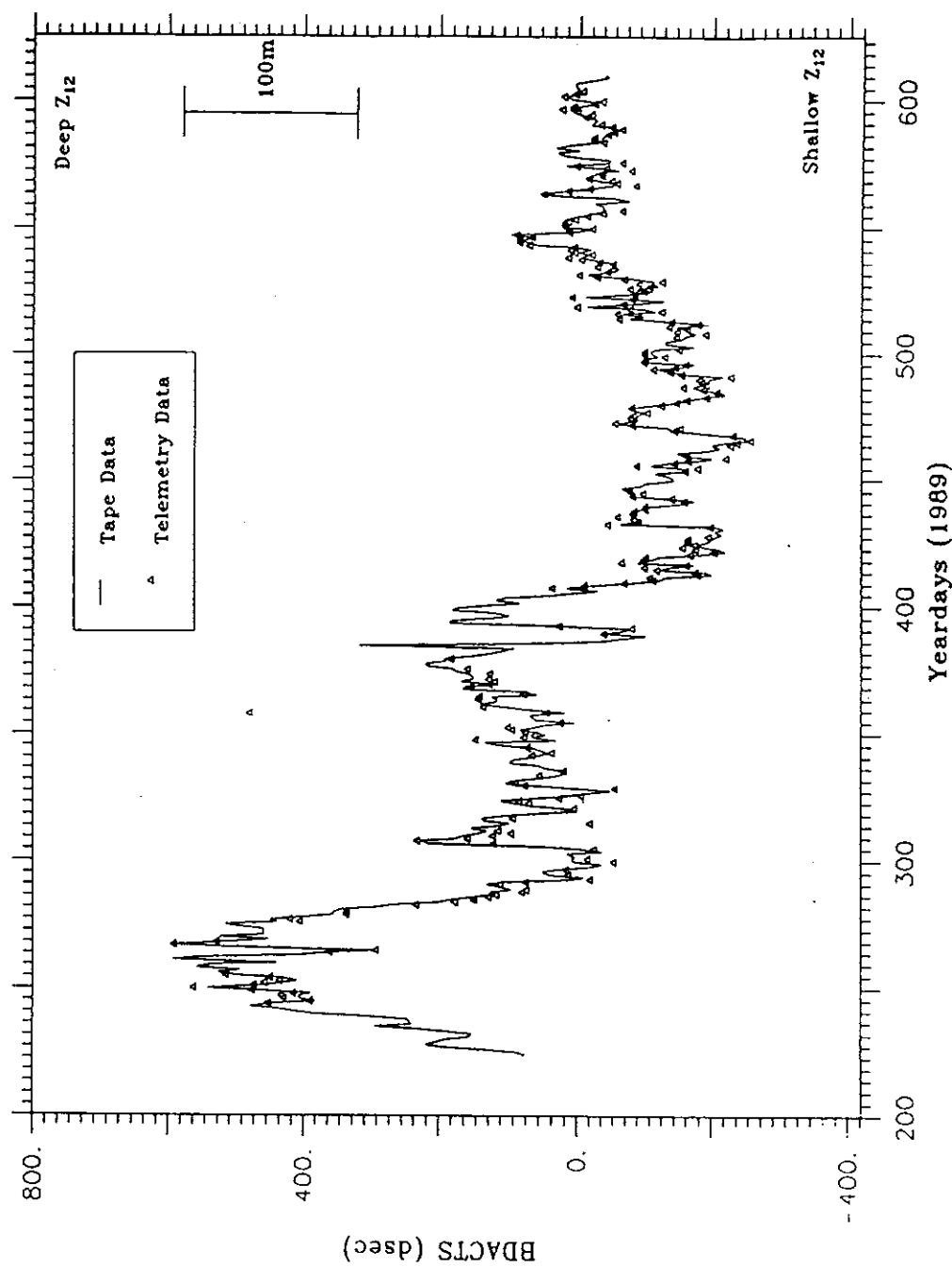


Figure 17: Comparison between the time delay as computed from the IES tape and that measured at Bermuda for IES B4. Both records have been independently despiked and demeaned.

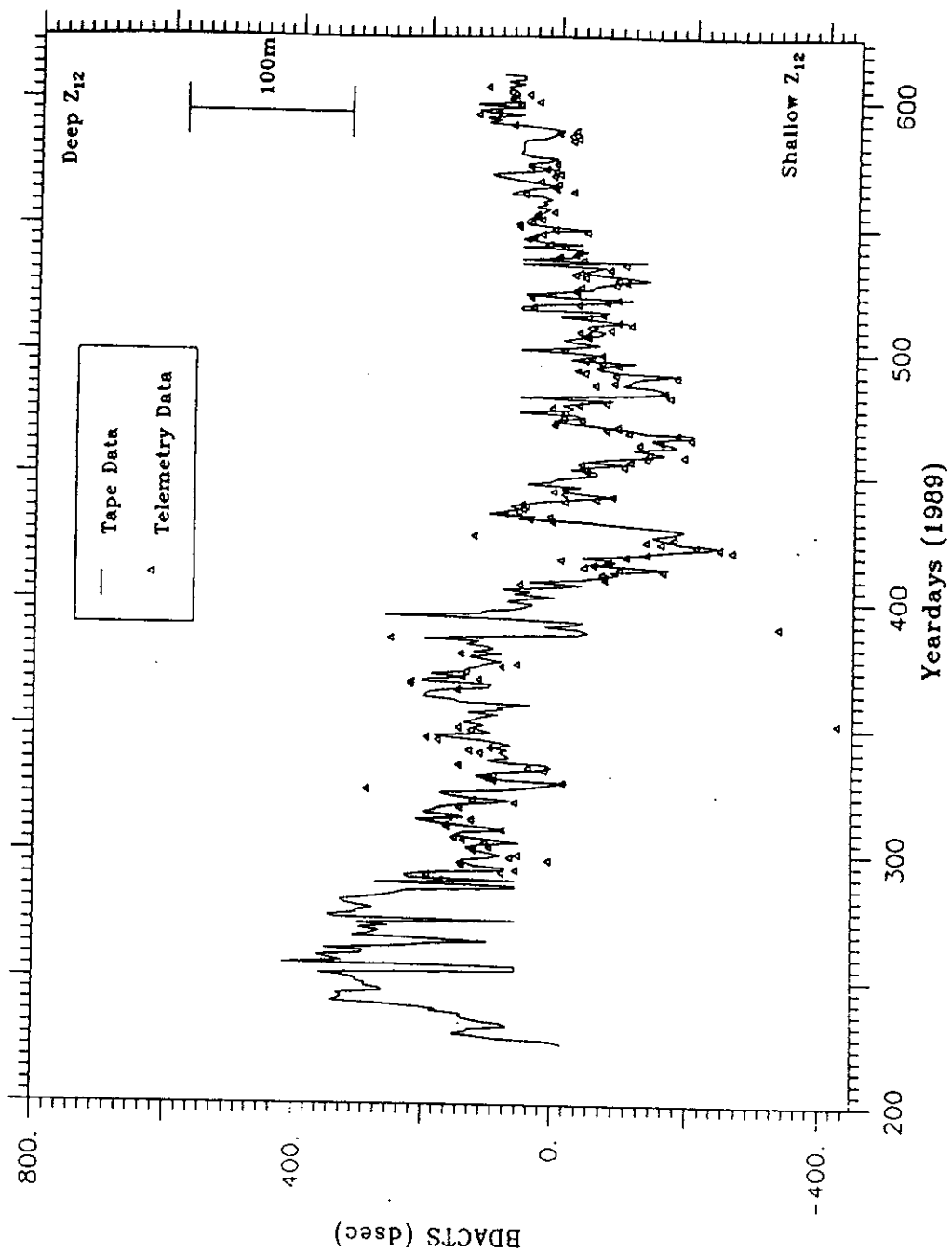


Figure 18: Comparison between the time delay as computed from the IES tape and that measured at Bermuda for IES B5. Both records have been independently despiked and demeaned.

Table 5: rms differences of BDACT between the tape and telemetry data. The values listed under Method 1 are computed after windowing the tape data and despiking the telemetry data separately. The values listed under Method 2 are computed after windowing out outliers in the daily difference between the tape and telemetry data delay times.

IES	Method 1		Method 2	
	rms (ds)	(m)	rms (ds)	(m)
B3	40	16	22	9
B4	35	14	22	9
B5	73	28	30	12

rms difference was 19 m. These differences can be attributed to the different type of processing performed on the various data sets.

In the previous section, we performed a "consistency check" by comparing the transmitted data with the received data (Comparison 1). We produced the time series records of transmitted data from the taped data using the same algorithm that the IES uses to calculate one  $\tau$  for each day and encode it for transmission. Ideally, the transmitted data and received data should agree perfectly. However, noise is introduced when data are transmitted over long distances. Thus, the rms differences reported in Table 5 represent how well the telemetry system itself worked.

In this section, the comparison is made between the tape and telemetered data which have been processed into  $Z_{12}$  independently of one another (Comparison 2). The tape travel times were processed using the steps described in Section 5.1, whereas the telemetry data were processed as described in Section 5.2. Although the processing steps perform essentially the same steps on the telemetered data, they are quite different in their implementation. For example, the half-hourly tape records are detided, low-pass filtered, and subsampled to produce  $Z_{12}$  time series with a 6-hr sample rate. Subsequently, the tape  $Z_{12}$  data are averaged to produce daily values. On the other hand, the data telemetered to Bermuda is a daily average and only requires low-pass filtering. (Recall that the taped and telemetered data are low-passed filtered with cutoff periods of 2-d and 4-d, respectively). The ordering of the averaging and the filtering steps results in the observed differences (Figure 19) between the tape and telemetered  $Z_{12}$  records.

It is not unreasonable to expect different processing methods to yield different results. So the rms values in Table 6 can be expected to be higher than those in Table 5, where the processing steps are identical. The importance of the values in Table 6 and the records in Figure 19 is that they describe how accurately the telemetry system works for monitoring the thermocline depth. Given the wide ranges in thermocline depth at each of the sites, Figure 19 shows that the telemetry system works very well.

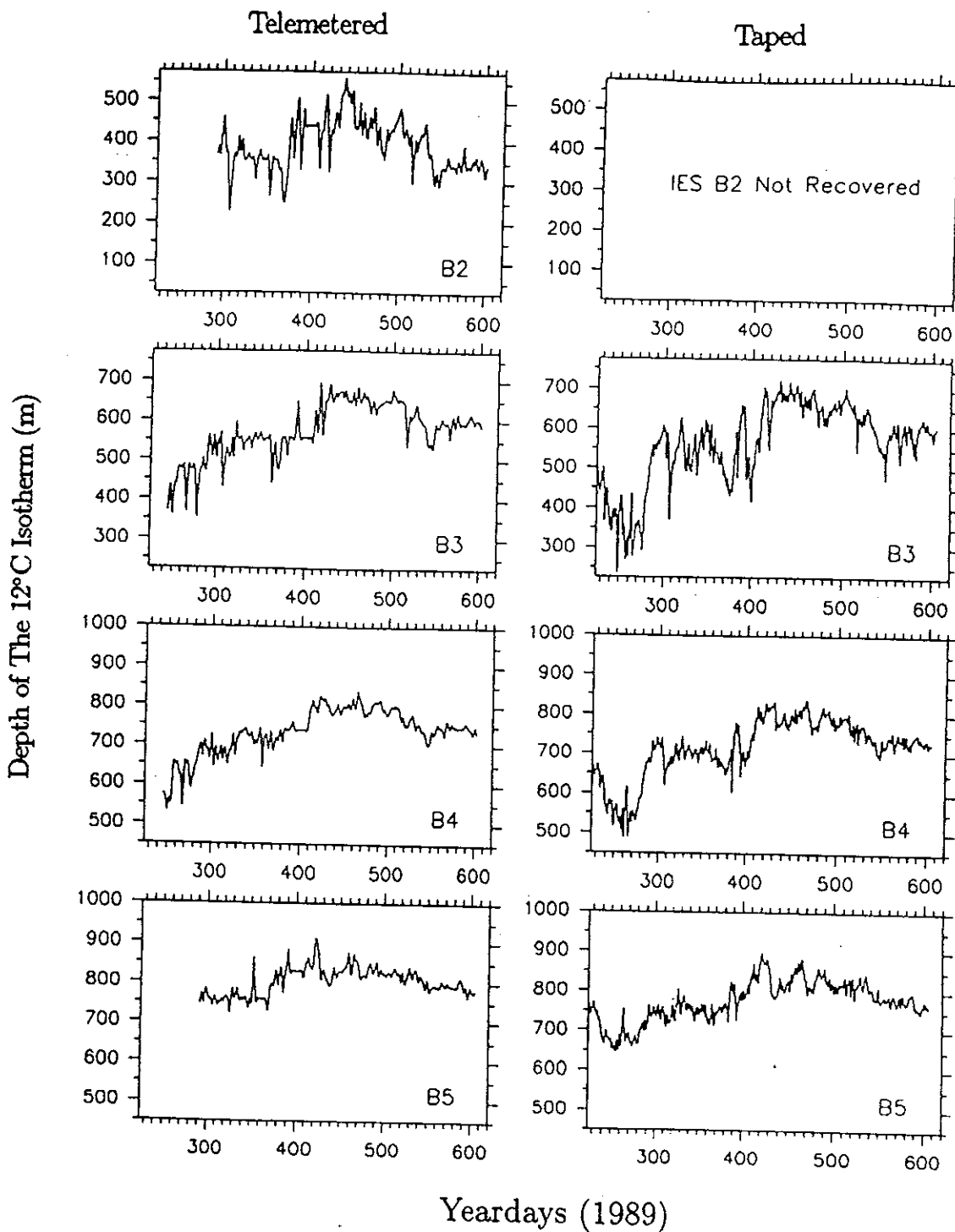


Figure 19: The column on the left shows the fully processed  $Z_{12}$  records from the telemetered data. The column on the right shows the corresponding records from the data on the IES tapes. The  $Z_{12}$  record from the tape data for IES B2 is not shown because the IES was not recovered.

Table 6: rms differences of  $Z_{12}$  between the tape and telemetry data. Column one shows the rms differences and column two shows the equivalent differences in ds or BDACT.

IES	Difference (rms) (m)	Difference (rms) (ds)
B3	38	98
B4	23	59
B5	26	67

$\left( \frac{5.9}{7.2} \right)^2$   
.82

## 6.5 Gulf Stream Position

Next we used the tape data and telemetered data to obtain the Gulf Stream North Wall (GSNW) position by 2 different techniques.

For the tape data, we performed our standard method by objectively mapping  $Z_{12}$  from the IESs in the SYNOP Inlet Array. The GSNW position along a line through the "B sites" was calculated from these maps as the position where  $Z_{12}$  was 350 m (note that our standard definition of the GSNW is where  $Z_{12}$  is 400 m, but  $Z_{12}$  at 350 m suffices for a comparison of the two data sets).

For the telemetered data a more simplistic approach for determining the GSNW position was used. Since the working telemetry IESs were moored along a line approximately perpendicular to the Gulf Stream path, a cross stream profile was used to determine the GSNW position using the technique of Watts and Johns (1982).

A comparison between the Gulf Stream North Wall (GSNW) position calculated from a common geographic position for both the tape and telemetered data is shown in Figure 20. For the telemetered data, on any given day, the GSNW position is determined from some combination of actual and filled  $Z_{12}$  values. The open triangles in Figure 20 show the GSNW position on days when there was at least one IES reporting "good data" (in this case the GSNW position is calculated from 1 actually measured  $Z_{12}$  and 3 filled  $Z_{12}$  values). Conversely, the solid triangles denote days when the GSNW position was calculated from 4 filled  $Z_{12}$  values. The low frequency signal shows good agreement except during the periods when the receiving station was down while the Gulf Stream moved rapidly onshore ( $\sim$  yeardays 255-265 and 267-275). The rms difference is less than 5 km between the tape and telemetered records for the Gulf Stream position for days in which good data was received from at least one IES. The 5 km rms is better than the  $\sim$ 10 km GSNW resolution from SST maps generated from AVHRR data. Thus, the telemetry system is an excellent method of obtaining real-time GSNW position through a limited domain mapped with IESs measuring main thermocline depth.

## 6.6 Telemetry System Problems

This was the first deployment of a telemetry system for real-time acquisition of IES data and the system concept was proven to work. However, as is frequently the case when things are done for the first time, a few problems occurred for which we have some proposed solutions.

As detailed earlier in Section 5.2.2, a very significant problem with the telemetry system occurred with the frequency settings of the IES internal clocks. Our frequency counter, used to measure the clock frequencies, was not calibrated correctly by the factory so our frequency measurements were in error. As a result, the telemetry records had time drifts which were translated into  $Z_{12}$  drifts by the data encoding scheme. The data could not be satisfactorily de-drifted until the IES data tapes were recovered. This drift problem could have been avoided by including a periodic zero-delayed signal from each IES. This signal could be used to keep track of any clock drift since such a drift would manifest itself as a departure of the arrival time of the signal from the expected time.

Gaps in the data were the result of both received data which were "bad" (rejected by the tests for bad data mentioned in section 5.2.3) and receiving station downtime. From the top panels of Figures 10-13 it is seen that the "bad" data were concentrated during a 70 day time span centered about yearday 360 of 1989. That is, the noisiest data were during the months of December through February, the time period of severest weather over the Sargasso Sea and Bermuda. At present, the only remedy for this problem is to interpolate between good values to fill in the gaps caused by the rejection of these points. The gaps resulting from the receiving station downtime are something that could have been almost entirely eliminated. Until an uninterruptable power supply (UPS) was added to the system, data were lost whenever the power went down (the power supply on Bermuda is not very stable). Data were also lost when problems arose with the modem used in the system. As pointed out in Section 6.1, the downtime of the receiving station was about 25 % so there is significant room for improvement.

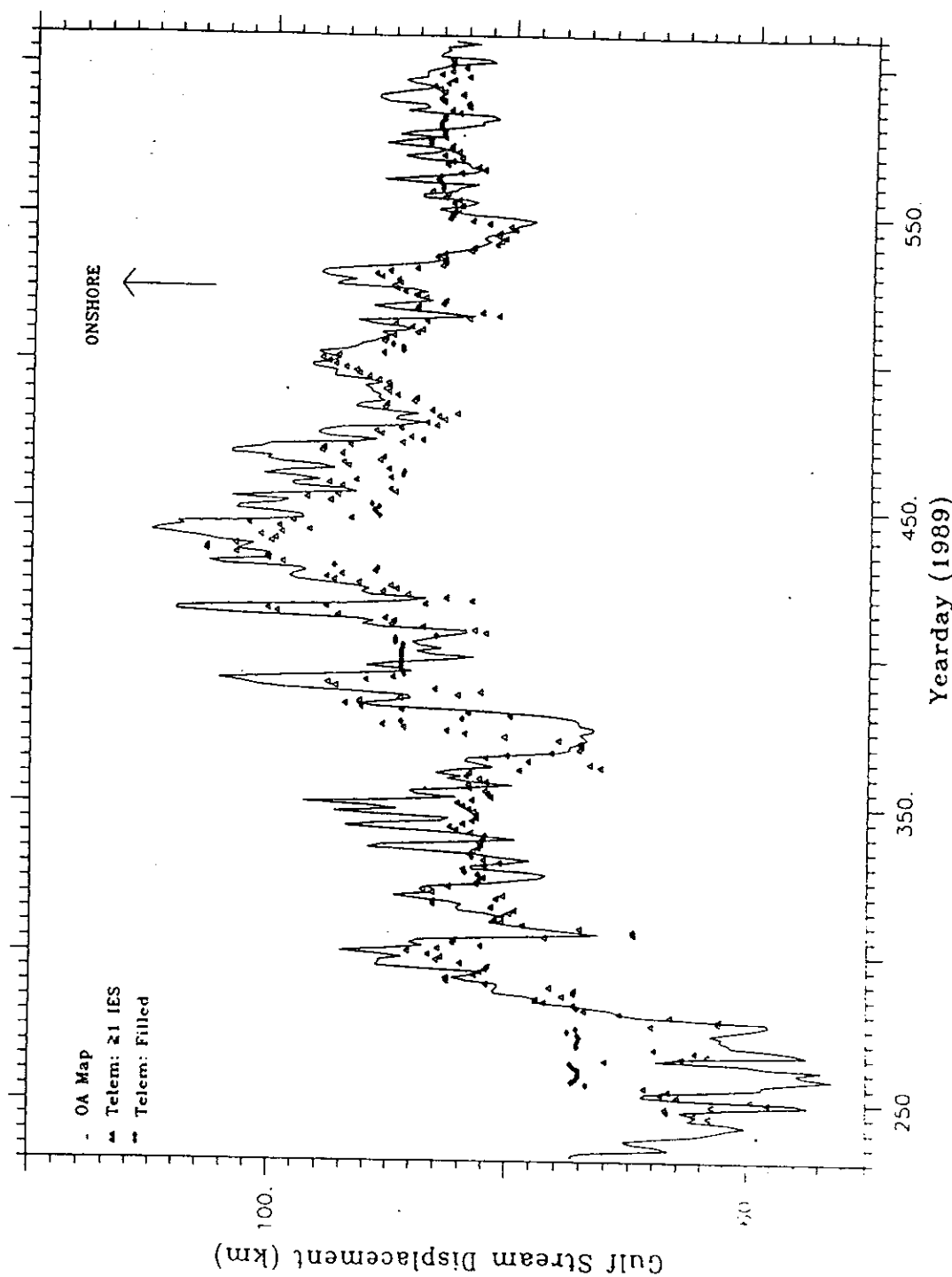


Figure 20: Gulf Stream North Wall displacement calculated from Objectively Mapped fields of  $Z_{12}$  in the SYNOP inlet array along the "B line" of IESs and from the telemetered data. The calculations are referenced to a common geographic position.

## 7 Summary and Conclusions

Despite the few avoidable problems encountered in the system, it has been shown that it is possible to obtain high quality IES data using an acoustic telemetry system. The average rms difference of 19 m between the data telemetered from the IESs and the data received at Bermuda is nearly the same as the average 20 m uncertainty in BINT calculations for IESs in our study area, Fields et al., (1991). This system was used for real time tracking of the Gulf Stream with accuracy of 5 km. The telemetry system is not limited to IESs, but could include similarly processed information from current meters, pressure gauges, ambient noise, etc. Such a system could be used in other regions where IESs are used (such as the Kuroshio) where there is a well defined sound channel.

## **8 References**

- Chaplin, G. 1990. Acoustic Telemetry System for Real-Time Monitoring of the Gulf Stream Path. *Proc. of Oceans.* 24-26 Sep. 1990. Washington, D.C., 1990.
- Howden, S. D., X. Qian, K. T. Tracey, and D. R. Watts. 1992. IES Calibration for Main Thermocline Depth: A Method Using Integrated XBT Temperature Profiles. *G. S. O. Technical Report in preparation*
- Fields, E., K. T. Tracey, and D. R. Watts. 1991. Inverted Echo Sounder Data Processing Report. *G. S. O. Technical Report No. 91-3.*
- Watts, D. R. and H. T. Rossby. 1976. Measuring Dynamic Heights with Inverted Echo Sounders. *J. Phys. Oceanogr.*, 7, 345-358.

(

(

(

(

(

(

(

(

(

(

(

## REPORT DOCUMENTATION PAGE

1a. REPORT SECURITY CLASSIFICATION Unclassified		1b. RESTRICTIVE MARKINGS	
2a. SECURITY CLASSIFICATION AUTHORITY		3. DISTRIBUTION/AVAILABILITY OF REPORT	
2b. DECLASSIFICATION/DOWNGRADING SCHEDULE			
4. PERFORMING ORGANIZATION REPORT NUMBER(S) University of Rhode Island Graduate School of Oceanography GSO Technical Report 91-8		5. MONITORING ORGANIZATION REPORT NUMBER(S)	
6a. NAME OF PERFORMING ORGANIZATION University of Rhode Island Graduate School of Ocean.	6b. OFFICE SYMBOL (if applicable) 1122 PO	7a. NAME OF MONITORING ORGANIZATION	
6c. ADDRESS (City, State, and ZIP Code) South Ferry Road Narragansett RI 02882		7b. ADDRESS (City, State, and ZIP Code)	
8a. NAME OF FUNDING/SPONSORING ORGANIZATION Office of Naval Research	8b. OFFICE SYMBOL (if applicable)	9. PROCUREMENT INSTRUMENT IDENTIFICATION NUMBER	
8c. ADDRESS (City, State, and ZIP Code) 800 No. Quincy Street Arlington VA 22217		10. SOURCE OF FUNDING NUMBERS	
		PROGRAM ELEMENT NO.	PROJECT NO.
		TASK NO.	WORK UNIT ACCESSION NO.
11. TITLE (Include Security Classification) Inverted Echo Sounder Telemetry System Report			
12. PERSONAL AUTHOR(S) Stephan Howden, Karen Tracey, D. Randolph Watts, H. Thomas Rossby			
13a. TYPE OF REPORT GSO Technical Rpt.	13b. TIME COVERED FROM 8/89 TO 9/90	14. DATE OF REPORT (Year, Month, Day) 1991 December	15. PAGE COUNT 42
16. SUPPLEMENTARY NOTATION			
17. COSATI CODES		18. SUBJECT TERMS (Continue on reverse if necessary and identify by block number) Gulf Stream, Inverted Echo Sounders, SYNOP Real-time Acoustic Telemetry, SOFAR Channel	
19. ABSTRACT (Continue on reverse if necessary and identify by block number)			
<p>From August 1989 until August 1990, a simple acoustic telemetry system was used for obtaining real-time data from 5 Inverted Echo Sounders (IESs) deployed in the SYNOP inlet array in the Gulf Stream east of Cape Hatteras. Every 24 hours, each IES calculated a representative travel time from a set of 48 measurements (<math>\tau</math>), and telemetered that value to a listening station on Bermuda. From the received data, a daily time series of the depth of the 12°C isotherm (our proxy for main thermocline depth) over each IES was calculated. The position of the Gulf Stream North Wall through the IES array was calculated on a daily basis from the thermocline depth information at each IES site.</p> <p>The telemetry system is based on encoding data as a time delayed broadcast acoustic signal: the delay of the time of broadcast of the signal, with respect to a reference time, is proportional to the data value. The changes in delay time, from one broadcast signal to the next, are recorded at a remote receiving station.</p>			
20. DISTRIBUTION/AVAILABILITY OF ABSTRACT <input checked="" type="checkbox"/> UNCLASSIFIED/UNLIMITED <input type="checkbox"/> SAME AS RPT. <input type="checkbox"/> DTIC USERS		21. ABSTRACT SECURITY CLASSIFICATION	
22a. NAME OF RESPONSIBLE INDIVIDUAL Stephan D. Howden		22b. TELEPHONE (Include Area Code) (401) 792-6514	22c. OFFICE SYMBOL

**Block 19 continued**

The IESs were recovered in August 1990, with the exception of the one at site B2. The telemetered data from the IES at site B2 was, however, received at Bermuda. The RMS agreement between thermocline depths, as calculated from the data on tape from the recovered IESs and as calculated from the received telemetry data, is 20 m. This compares favorably with the 19 m uncertainty in calibrating the  $\tau_s$  as a measure of the thermocline depth. The RMS agreement between the position of the Gulf Stream path through the IESs as calculated from the tape data and the telemetry data is 5 km.

This telemetry system is not IES specific. It could be used with other appropriately modified oceanographic instruments, such as current meters and pressure sensors.